On Prefabricated Vertical Drain (PVD) and Deep Cement Mixing (DCM) / Stiffened DCM (SDCM) Techniques for Soft Ground Improvement

D. T. Bergado[1], P. V. Long[2], P. Jamsawang[3], C. Na Lampun[4], and A.S. Balasubramaniam[5]
[1]*Professor Emeritus, Asian Institute of Technology and Geotechnical Specialist, Index International Group, Bangkok, Thailand*
[2]*President and CEO, Vina Mekong Consultants (VMEC), Ho Chieh Minh City, Vietnam*
[3]*Associate Professor, King Mongkut's University of Technology North Bangkok (KMUTNB), Bangkok, Thailand*
[4]*President and CEO, Index International Group, and Hon. Doctorate, Kasetsart University, Bangkok, Thailand*
[5]*Emeritus Professor, Asian Institute of Technology, Bangkok, Thailand and Adjunct Professor, Griffith University, Gold Coast Campus, Brisbane, Australia*
[1]*E-mail:* dbergado@gmail.com

ABSTRACT: Soft ground improvement techniques have become most practical and popular methods to increase soil strength, soil stiffness and reduce soil compressibility including the soft Bangkok clay. This paper focuses on comparative performances of prefabricated vertical drain (PVD) using surcharge, vacuum and heat preloading as well as the cement-admixed clay of Deep Cement Mixing (DCM) and Stiffened DCM (SDCM) methods. The Vacuum-PVD can increase the horizontal coefficient of consolidation, C_h, resulting in faster rate of settlement at the same magnitudes of settlement compared to Conventional PVD. Several field methods of applying vacuum preloading are also compared. Moreover, the Thermal PVD and Thermal Vacuum PVD can increase further the coefficient of horizontal consolidation, C_h, with the associated reduction of k_h/k_s values by reducing the drainage retardation effects in the smear zone around the PVD which resulted in faster rates of consolidation and higher magnitudes of settlements. Furthermore, the equivalent smear effect due to non-uniform consolidation is also discussed in addition to the smear due to the mechanical installation of PVDs. In addition, a new kind of reinforced method, namely: Stiffened Deep Cement Mixing (SDCM) pile is introduced to mitigate the problems of the Deep Cement Mixing (DCM) pile due to the low flexural resistance, lack of quality control in the field and, consequently, unexpected failures. The SDCM pile consists of DCM pile reinforced with precast reinforced concrete (RC) core pile. The full scale test embankment on soft clay improved by SDCM and DCM piles was studied. Numerical simulations using the 3D PLAXIS Foundation finite element software have been done to understand the behavior of SDCM and DCM piles. The simulation results indicated that the surface settlements decreased with increasing lengths of the RC core piles, and, at lesser extent, increasing sectional areas of the RC core piles in the SDCM piles. In addition, the lateral movements of the embankment decreased by increasing the lengths (longer than 4 m) and, the sectional areas of the RC core piles in the SDCM piles. The results of the numerical simulations closely agreed with the observed data and successfully verified the parameters affecting the performances and behavior of both SDCM and DCM piles.

KEYWORDS: Ground improvement, PVD, DCM pile, SDCM pile, Soft clay, Laboratory test, Full scale test.

1. INTRODUCTION

Prefabricated vertical drains (PVDs) is the cheapest method of soft ground improvement, this is the reason why the PVD method has widely adopted and applied for construction on soft ground (Hansbo, 1979, 1981; Bergado et al., 2002; Abuel-Naga et al, 2015). PVDs with embankment preloading method functions by draining the pore water mostly in horizontal direction from the surrounding soft soil faster during the consolidation process by shortening the drainage path and by taking advantage of the higher horizontal hydraulic conductivity in the soft ground deposit. Then, the pore water can flow freely along the drain vertically towards the permeable drainage layers. However, the PVD installation using a mandrel causes disturbances in the clay surrounding the PVD resulting in lower horizontal hydraulic conductivity in the smear zone. (Hansbo, 1979, 1981; Bergado et al., 1991; Abuel-Naga and Bouazza, 2009). PVDs with embankment preloading combined with vacuum pressure (called Vacuum PVD) has been utilized to minimize the instability problem and to accelerate the rate of consolidation. Kjellman (1952) first proposed the vacuum consolidation in early 1950s. Subsequently, the studies of vacuum consolidation continued up to the present (Chai et al, 2006, 2008; Saowapakpiboon et al, 2009, 2010; Lam et al, 2015; Long et al, 2015,2016). Vacuum consolidation can reduce the pore pressure and maintain constant total stress instead of increasing the total stress. The effective stress is increased due to the reduced (less than atmospheric) pressure in the soil mass. In addition, with heat application, the horizontal hydraulic conductivity in smear zone, k_s, around the PVD increased which was first proposed by Abuel-Naga et al. (2006). This technique is called Thermal PVD by using the thermal treatment up to 90˚C combining with PVD. The PVD combined with heat works by the reduction of the smear effect due to the increased clay permeability at elevated temperature. Consequently, faster rate of consolidation was achieved but with larger magnitude of settlement (Pothiraksanon et al., 2008). The effect of temperature on the soil permeability was also studied previously and reported that the hydraulic conductivity of soil increased with increasing the temperature (Abuel-Naga et al, 2006, 2007). The effect of heat on the volume change and compressibility of clays were also studied (Abuel-Naga et al, 2008).

Moreover, the one kind of ground improvement, which is continuously developed, is Deep Cement Mixing (DCM) pile. Although DCM pile has many advantages with various applications, failure caused by pile failure can occur especially when subjected to the lateral loads. Moreover, the unexpected lower strength than the design commonly occurs due to lack of quality control during construction. Thus, DCM pile still fails by pile failure mode which is lower than the soil failure mode particularly at the top of DCM pile due to low strength and stiffness (Petchgate et al, 2003). Consequently, the bearing capacity of DCM pile can be lower than the design load of 10 tons due to pile failure. Both pile and soil failures are illustrated in Fig. 35a.

To mitigate the failure problem, a new kind of composite pile named Stiffened DCM (SDCM) pile has been developed. This composite pile is composed of an inner precast concrete pile hereinafter called concrete core pile and an external DCM pile socket, where the high strength concrete pile is designed to bear the load, and DCM pile socket acts to transfer the axial force into the surrounding soil by skin friction.

The purposes of this study were to investigate the applicability of using the vacuum pressure combined with higher temperature up to 90°C combined with PVD as a ground improvement technique in reducing the smear effect and enhancing the PVD performance. The large scale method test was conducted to demonstrate the benefit of the vacuum pressure and thermal preloading compared with Conventional PVD. Subsequently, the performances of Conventional PVD, Vacuum PVD and Thermal PVD were evaluated and confirmed in the field full scale tests (Saowapakpiboon et al, 2010). In addition, the acceptance of numerical simulations in geotechnical problems is growing and finite element methods are increasingly used in the design of pile foundations. The full scale tests results were further simulated in order to study the parameters that affect the behavior of both the SDCM and DCM piles under the axial compression and lateral pile load as well as embankment load tests. Subsequently, the confirmed and verified parameters were used in the numerical experiments. Previously, the results of laboratory investigations of SDCM and their numerical simulations by Jamsawang et al. (2008) yielded useful parameters. The previous results served as the basis for the full scale pile load and embankment tests. Subsequently, numerical simulations were performed by Suksawat (2009) to back-calculate the strength parameters as well as to perform parametric study. Consequently, the results are presented in this paper.

2. PREFABRICATED VERTICAL DRAIN (PVD)

2.1 Laboratory tests using PVDs, Vacuum PVDs and Thermal PVDs

2.1.1 Large consolidometer

The large scale consolidometer (Figure 1) consisted of a cylinder cell of 0.45m in inner diameter and 0.95m in height made of polyvinyl chloride (PVC) with a thickness of 10 mm rested on steel base which can resist pressure less than 500 kPa. The air pressure was applied through the upper pedestal to the top of the piston and the vacuum pressure is applied through the shaft of the piston to the bottom of piston and the PVD cap, respectively. Air pressure was transformed to vacuum pressure by a vacuum generator which was connected directly with an air pump during consolidation test. A natural rubber membrane with a thickness of 3mm was installed in the chamber above the piston to prevent the leakage of the air pressure and/or vacuum pressure through the piston.

Figure 1 Large scale consolidometers for Thermal PVD and Thermal Vacuum PVD

The natural rubber membrane was folded in vertical direction initially to allow the vertical displacement of the piston during consolidation. Geotextiles were placed on top and bottom of the soil specimens to prevent clogging of the loading piston. Dial gauges were placed on top of the shaft for settlement measurements. A pore pressure transducer was installed and connected with data logger to monitor pore pressure in the specimen during consolidation.

Flexible heater wire with a capacity of 120°C and power of 6W per meter was attached to the PVD for the reconstituted specimen improved with Thermal PVD and Thermal-Vacuum PVD. Thermocouples were installed at radial distances of 25, 50, 100 and 200 mm and were connected to the digital data logger to monitor the temperature and heat transfer during the consolidation test (Figure 2). Before and after the laboratory tests, the water contents and shear strengths were also measured at the aforementioned locations, the temperature sensor boxes were used to maintain the heat temperature at heat source and shut down automatically upon reaching the controlled heat of 90°C, at the heat source.

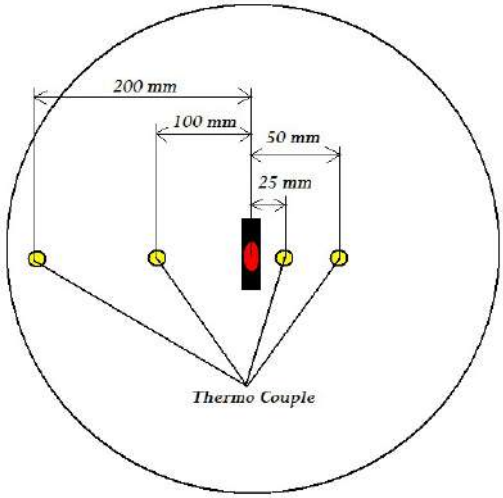

Figure 2 Configurations of PVD and thermo couples (not to scale)

Customized vane shear equipment was used to measure the undrained shear strength before and after consolidometer tests. The vane blade made of stainless steel, is 20mm in diameter and 40mm in height. It is attached to an adjustable stainless steel rod 5mm in diameter, capable of measuring the shear strengths at different locations and depths. The rod was held in place by a removable rectangular steel adapter above the circular plate rotator. The adapter was connected to the force sensor, which was attached on top of the circular rotator when the vane is turned. The force sensor was connected to the transducer to determine the readings. The maximum torque of each radial distance was calculated by multiplication of force and radial arm distance. The vane shear tests were done at radial distances of 25mm, 50mm, 100mm and 200mm, respectively, at two different depths.

The vacuum generator was utilized to transform the air pressure to vacuum pressure. This apparatus was connected directly with air pump during consolidation test. The water generated from suction by vacuum pressure was stored in a closed container.

A KPD-200 kPa excess pore pressure transducer was connected with data logger to monitor the pore pressure in the specimen during consolidation using a probe inserted into the wall of the consolidometer cell at the desired level. The excess pore pressures were monitored in the consolidomer test by using the data logger.

2.1.2 Test procedures

The soil samples used in this study were obtained from a site which is located at the area of Second Bangkok International Airport

(SBIA), Thailand. The soft clay samples were collected from 3.0 to 4.0m depths. Disturbed samples were obtained by digging the soils up to required depth with a backhoe. Then, the disturbed soil samples were placed in covered plastic containers for storage. Undisturbed samples were collected by 10 inches piston samples and immediately covered with wax after sampling to prevent loss of moisture. The physical properties of the soft Bangkok clay are shown in Table 1. The PVD material used was CeTeau drain (CT-D911). The disturbed samples were mixed by using a mixer. Water was added until the water content was slightly greater than the liquid limit. The mixed soil was placed into the large scale consolidometer cell layer by layer until to the desired height. The appropriate loads were applied for the reconstitution process to obtain the desired water content and void ratio equal to the initial conditions.

Table 1 Physical properties of soft Bangkok clay in Suvarnabhumi Airport

Physical properties	
Liquid limit (%)	102.24
Plastic limit (%)	39.55
Water content (%)	112.69
Plasticity index	62.69
Total unit weight (kN/m^3)	14.70
Specific gravity	2.66

2.1.3 Consolidometer test program

For the reconstitution using the new large consolidometer, a 50 kPa pressure was applied. Drainage was allowed to flow to the top and bottom of the apparatus. Silicone grease was applied to the insides of the large consolidometer to reduce the friction. Throughout the whole process, the settlements were monitored. After reconstitution, the water content, shear strength, and specimen height were determined. The vertical pressure of 50 kPa was increased to 100 kPa after reconstitution under the applied vertical pressure in the specimen improved with PVD. For the specimen improved with PVD and vacuum pressure (Vacuum PVD), a vertical pressure of 50 kPa and vacuum pressure of -50 kPa were applied. For the Thermal PVD, the specimen was improved with PVD combined with vertical pressure of 100 kPa together with application of heat up to 90 ºC. For the Thermal Vacuum PVD, the specimen was improved with PVD combined with heat up to 90 ºC together with vertical pressure of 50 kPa and vacuum pressure of -50 kPa. The temperatures were controlled by an electronic thermal control unit that received the signal from thermocouples. Drainage was allowed to flow only one way. Settlement was monitored during the test until the soil specimen reached to 90% consolidation. The method of Asaoka (1978) was used to estimate the degree of consolidation and the magnitude of final settlement. The large scale consolidometer tests of specimens improved with Conventional PVD, Vacuum PVD, Thermal PVD and Thermal Vacuum PVD are shown in Figure 1.

2.1.4 Effect on the coefficient of consolidation, C_h, and permeability ratio, k_h/k_s

The values of C_h for all tests were back-calculated using the equations from Hansbo (1979) for radial consolidation with PVD is given as follows:

$$U_h = 1 - \exp\left[\frac{-8T_h}{F}\right] \quad (1)$$

where U_h is the degree of consolidation for horizontal drainage; T_h is the time factor for horizontal drainage; *F* is the factor which expresses the additive effect due to the spacing of the drains, F(n), smear effect, F_s, and well-resistance, F_r. The values of F(n), F_s and F_r are given by the following equations:

$$F(n) = \ln\left[\frac{D_e}{d_w}\right] - \frac{3}{4} \quad (2)$$

$$F_s = \left[\frac{k_h}{k_s} - 1\right] \ln\left[\frac{d_s}{d_w}\right] \quad (3)$$

$$F_r = \pi z(L - z)\frac{k_h}{q_w} \quad (4)$$

where D_e is the diameter of the equivalent soil cylinder, d_w is the equivalent diameter of the drain, k_h is the coefficient of horizontal permeability, k_s is the horizontal permeability of the smear zone, d_s is the diameter of the smear zone, z is the distance from the drainage end of the drain, L is the length of the drain for double drainage and twice the length of the drain for single drainage, q_w is the discharge capacity of the drain at hydraulic gradient of 1 (one). The time factor, T_h, for horizontal drainage can be calculated using:

$$T_h = \frac{C_h t}{D_e^2} \quad (5)$$

where C_h is the coefficient of horizontal consolidation and t is the time elapsed after the application of the load.

2.1.5 Consolidation behavior of tested samples

The comparison of settlements of specimens improved with and without vacuum and heat in the large scale consolidometers test are shown in Figure 3. The specimen improved with Vacuum PVD has higher rate of settlement than the specimen improved with Conventional PVD but the final settlement magnitudes are the same. In contrast, much faster and higher settlements were achieved from Thermal PVD and Thermal Vacuum PVD. However, the performance of Thermal PVD is slightly lower than Thermal Vacuum PVD. Among the tests, the Thermal Vacuum PVD combination achieved the fastest rate of settlement and the largest final settlement. There is 25% of increase in final settlement in Thermal PVD with almost the same settlement magnitude with the Thermal Vacuum PVD. Similar results to Pothiraksanon et al. (2010), the use of the Thermal PVD result in increased settlements of about 30%. In addition, Saowapakpiboon et al. (2010) showed the differences in the rate of settlement of Thermal PVD was highest due to volume contraction and rate of consolidation due to thermal effects. These results show that the higher the temperature, the higher the volume contraction and the higher the rate of consolidation resulting from the increased soil permeability due to reduced pore water viscosity (Abuel-Naga et al, 2007). The compressibility increases due thermally induced irreversible contraction of saturated normally consolidated soft Bangkok clay. Furthermore, Abuel-Naga et al. (2006) indicated substantial increase in the clay permeability up to more than 3 times when the temperature was raised up to 90 degrees centigrade under fully drained constant stress conditions oedomoter tests in the laboratory. Moreover, the compression line of soft Bangkok clay shifts to the left with approximately similar slope upon heating when the thermal loading is applied at normally consolidated state (Abuel-Naga et al.

2008). Thus, heating the clay specimen combined with both heat and vacuum pressure (Thermal Vacuum PVD) has achieved the highest settlement and also faster rate of consolidation than Thermal PVD, Vacuum PVD and Conventional PVD, respectively.

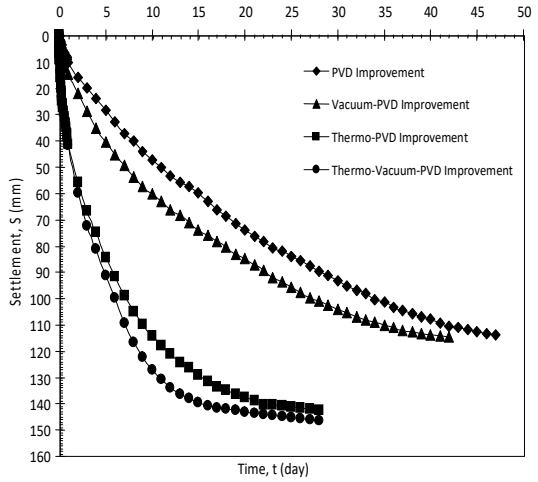

Figure 3 Comparison of settlement behavior using large consolidometer with reconstituted specimen

2.1.6 Heat transfer

The heat transfers in the soil specimens at specific temperatures with respect to the specific distances from PVD were observed. Flexible wire heaters attacked to the core of PVD were used as heat source to increase the temperature up to 90ºC. Temperatures of the heat source were measured by thermocouples which were embedded at 150mm depth and at radial distances of 25mm, 50mm 100mm and 200mm from the center of the specimen. The temperature decreased with distance from the heat source. The Thermal Vacuum PVD has similar heat transfer characteristics with the Thermal PVD. The radius, r, of 25 mm corresponds to the location of the smear zone with a mandrel dimension of 18.2 mm x 81.90 mm, and the diameter of the disturbed zone can be calculated as 87mm. Figure 4 shows the temperature of 80 ºC in the smear zone and decreased with distance from the heat source. It took 40 hours for the temperature to reach equilibrium in the large consolidometer. The result is consistent with the previous work of Abuel-Naga, et al. (2006). The temperature change around the PVD decreased as the radial distance increased and become constant thereafter.

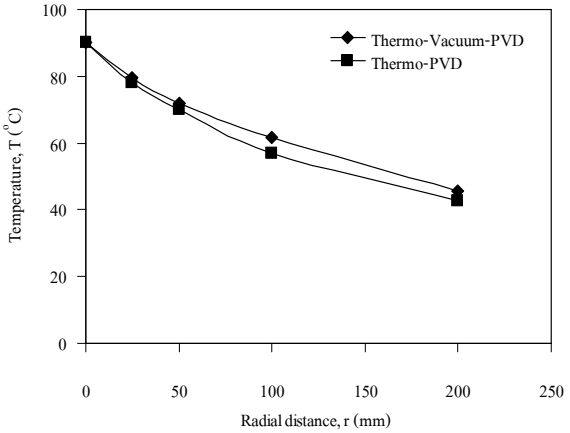

Figure 4 Comparison of temperatures with radial distances in Thermal PVD and Thermal Vacuum PVD

2.1.7 Vacuum and thermal effect on water content

The reduction in water content was measured before and after consolidation tests at the radial distances of 25mm, 50mm, 100mm and 200mm from the center of the specimens at depths 10 mm and 40 mm. Lower water contents were observed nearer to the heat source with significant reduction in water contents. The levels of water content reduction decreased with the distance from the heat source. The percent decrease of water contents after consolidation tests at the smear zone of Vacuum PVD was slightly higher than that Conventional PVD. The Thermal PVD had much higher percent decrease of water contents than the Vacuum PVD while the Thermal Vacuum PVD had the highest percent decrease of water contents but nearly similar to that of Thermal PVD**.**

2.1.8 Effect of vacuum and heat on shear strength of clay

A comparison of the increase in the shear strength in all the four tests after improvement in the reconstituted specimens is plotted in Figure 5. For the smear zone, the Conventional PVD and Vacuum PVD were not much different in the increase of shear strengths. For Thermal PVD, the shear strength had increased but slightly less than the Thermal Vacuum PVD around the smear zone. The results demonstrated that much higher shear strength developed in the smear zone using Thermal PVD and Thermal Vacuum PVD. The increase in shear strength is due to the reduction of water contents and because the clay particle changed to flocculated structure with volume contraction as the soil temperature increased (Abuel-Naga, et al, 2008).

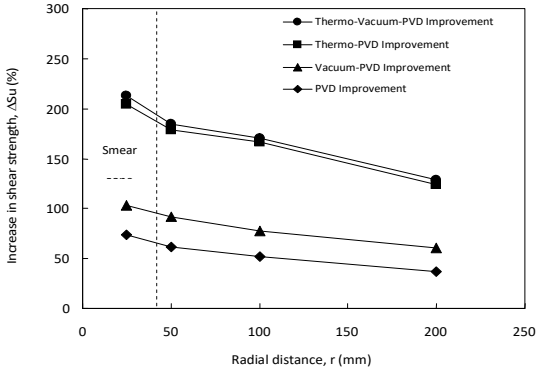

Figure 5 Comparison of increase in shear strengths (%) with radial distances after consolidation test

2.1.9 Vacuum and thermal effects on excess pore pressure

The excess pore pressures were measured at the large scale consolidometer tests during consolidation by using excess pore pressure transducers which were inserted through the wall of the cylinder cell into the smeared and undisturbed zone and monitored by digital data logger. For specimen with Conventional PVD, the excess pore pressure had increased to maximum of 80 kPa and decreased to about 10 kPa after 47 days in the undisturbed zone. For Thermal PVD, the specimen at the undisturbed zone had demonstrated higher excess pore water pressures to 80 kPa and then rapidly reduced to 1 kPa after 28 days due to the effects of thermally induced pore water pressures and volume changes. This behavior demonstrates that the permeability in the smear zone was increased at higher temperature. Consequently, the excess pore water pressures dissipated more rapidly (Pothiraksanon et al., 2010). The thermally induced excess pore pressures were larger because the thermal expansion coefficient of the pore water is approximately 15 times larger than the thermal expansion of the clay solid skeleton (Abuel-Naga, et al., 2007). In the case of, Vacuum PVD specimen, the maximum excess pore pressure in the smear zone had increased

about 40 kPa and dissipated rapidly after 8 days and decreased to about -40 kPa after 40 days. The excess pore pressures in the undisturbed zone increased to maximum of 40 kPa and transformed to minus excess pore pressure after 13 days and decreased to about -40 kPa after 40 days. The excess pore pressure had reduced faster at the smear zone than in the undisturbed zone due to the proximity to vacuum source. The excess pore pressure of Thermal Vacuum PVD specimen in the undisturbed zone increased to 40 kPa and reduced very fast to -9.1 kPa after only 6 days and then decreased to about -43 kPa after 28 days. The vacuum preloading generates negative (suction) excess pore pressure equivalent to the applied vacuum pressure. This behavior is similar to the results of Indraratna et al. (2005) which indicated that the assumption of constant vacuum pressure distribution over the soil surface and linearly decreasing vacuum pressure along the drain length. Moreover, Chai et al. (2007b) showed the measured and simulated excess pore pressure and vacuum pressure variation with time. The simulated values and dissipation rates were higher than the measured values.

2.1.10 C_h and k_h/k_s values

The test results from reconstituted specimens in the large scale consolidometer were back-calculated to determine the values of C_h and k_h/k_s by using the method by Hansbo (1987). The back-calculated values of reconstituted specimen improved with Conventional PVD obtained C_h value of 1.93 m^2/yr with k_h/k_s of 3.0. For reconstituted specimen improved with Vacuum-PVD, the back-calculated C_h value consisted of 2.23 m^2/yr with k_h/k_s of 2.7. Similar results were observed by Mohamedelhassan and Shang (2002) wherein the vacuum and surcharge preloading of the same magnitudes produced similar amounts of compression. Recently, Lam et al (2015) presented numerical and analytical analyses of field data from Conventional PVD and Vacuum PVD while Long et al (2015, 2016) presented field results of Vacuum PVD with and without airtight membranes. Meanwhile, Chai and Rondonuwu (2015) has investigated the effects of surcharge loading rate for minimizing the lateral displacement of Vacuum PVD improved soft clay.

Similarly, for the reconstituted sample in large consolidometer with heat (Thermo-PVD), the corresponding back-calculated C_h and k_h/k_s are 4.17 m^2/yr and 1.4, respectively. These values show that the thermal effects increased the permeability of the smear zone resulted in the decrease k_h/k_s values and increase in the C_h values. Due to the elevated temperature, the viscosity of the pore water decreased and the soil permeability increased in the smear zone (Abuel-Naga, et al., 2009). Moreover, for the reconstituted specimen improved with Thermal Vacuum PVD, the C_h and k_h/k_s are 4.38 m^2/yr and 1.1, respectively. The predicted curve agreed well with the observed values of reconstituted specimens in large scale consolidometer tests. In summary, the values of the C_h and k_h/k_s for all the specimens are also tabulated in Table 2. The percent increases in C_h of the reconstituted specimen improved with Vacuum PVD, Thermal PVD and Thermal Vacuum PVD consisted of 15.5%, 116.1% and 126.4% respectively. The reductions in k_h/k_s were 10.0%, 53.3% and 63.3%, respectively. Thus, the vacuum pressure can increase the horizontal coefficient of consolidation, C_h because the vacuum pressure generated negative pore water pressure along the drain so the effective stress of soil increased which resulted in faster rate of settlement with the same magnitudes of settlement compared to Conventional PVD (see Figure 3). The high temperature can further increase the coefficient of horizontal consolidation, C_h with the reduction of k_h/k_s because the soil permeability increased and consequently reduced the drainage retardation effects in the smear zone around the PVD. Moreover, the soil elements also changed the volume of particle arrangement from the thermal effect with much faster rates of consolidation and higher magnitudes of settlement (Abuel-Naga et al 2007).

Table 2 Summary of changes in flow parameters for reconstituted specimens using large consolidometer

Flow parameters	PVD	Vacuum-PVD	Thermo-PVD	Thermo-Vacuum-PVD
C_h (m^2/yr)	1.93	2.23	4.17	4.38
k_h/k_s	3.00	2.70	1.40	1.10

2.2 Field test using PVDs with and without vacuum pressure

2.2.1 Site investigations and field construction

Both vacuum-PVD and conventional PVD system at Suvarnabhumi Airport, Thailand were reported by COFRA (1996). The soil profile at the site can be divided into 8 sublayers as shown in Table 3 and it consists of a 2.0 m thick weathered clay layer overlying a very soft layer which extends from 2.0 m to 10.0 m depth. Underneath the soft clay layer of 3.0 m thickness, a 3.0 m thick medium clay layer can be found. The light-brown stiff clay layer can be encountered at 15.0 m to 30.0 m depth. The groundwater level was found at about 0.50 m depth. In Table 3, the maximum past pressure (POP) is derived from the given OCR value taken as an average value of each layer. C_a is the coefficient of secondary consolidation. The soil profiles within the site are relatively uniform with some small variations in the soil thickness. The typical soil properties is also given in Figure 6 taken from Bergado et al (2002).

Table 3 Compressibility parameters at Suvarnabhumi Airport.

Type	Unit weight [kN/m^3]	Compressibility			POP (kPa)	C_v theory [m^2/yr]
		RR	CR	C_a		
weathered clay	18.50	0.035	0.350	0.014	45	-
very soft clay1	13.80	0.050	0.500	0.020	37	0.79
very soft clay2	14.00	0.042	0.420	0.017	59	0.79
soft clay	15.00	0.040	0.400	0.016	100	0.79
soft to medium clay	15.70	0.030	0.300	0.012	110	0.79
stiff clay1	18.50	0.008	0.080	0.003	300	-
stiff clay2	19.00	0.008	0.080	0.003	500	-
stiff clay3	20.40	0.000	0.000	0.000	500	-

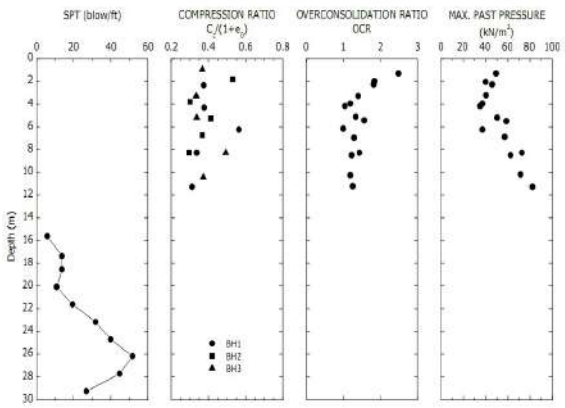

Figure 6 Soil parameters of SBIA project (Bergado et al, 2002)

In the Conventional PVD method, the PVD was installed to 10 m depth with a spacing of 0.85 m and arranged in a triangular pattern. This method had the embankment height in 4.2 m with loading in 2 stages.

Typically, a 2:1 side slope was used for the low embankment with height less than 2.5 m. However, a 4:1 side slope was adopted for the high embankment to reduce the effect from erosion due to rainfall. The high embankment is usually constructed along with counterweight berms for stability purpose. The cross-section of the test embankment using conventional PVD method is shown in Figure 7. Several types of monitoring instruments were used, including settlement plates, settlement benchmark, deep settlement gauges, piezometers, inclinometers and observation wells. It is worth to mention that Abuel-Naga et al (2006) has devised a design chart for Conventional PVD incorporating varied soil permeabilities in the smear zone.

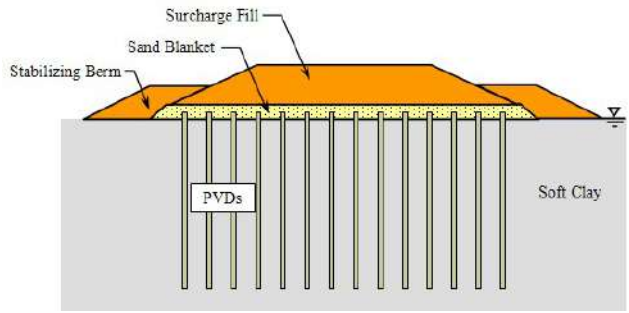

Figure 7 Cross-section of test embankment using conventional PVD method

VCM-DT method - Vacuum PVD method using direct connection method without airtight membranes, the PVD was installed into 10 m depth with a spacing of 0.85 m and arranged in a triangular pattern. The instrumentation equipments were installed to monitor the field behavior. For the vacuum-PVD, similar instrumentation equipments were installed to monitor the field behavior. The locations of the inclinometers, piezometers and the settlement plate are shown in Figure 8. The following boundary conditions were used in the design of vacuum-PVD: installation time of drains of 2 months, maximum pumping time of 8 months, vacuum pressure of -60 kPa at 5 m depth, depth or length of PVD of 10 m below ground surface and 60 % consolidation requirement. The embankment was 2.8 m high with unit weight of 18 kN/m^3. The embankment was constructed in two phases, namely: Phase 1 (1.5 m height, day 0) and Phase 2 (1.3 m height, day 14). The load-time relations of PVD improvement with and without vacuum preloading are shown in Figure 9.

Herein, the Vacuum PVD system used the direct connection method without sealing geomembranes at the ground surface. Long et al (2015, 2016) has presented full scale case histories of Vacuum PVD with and without airtight membranes. Chai and Rodonuwu (2015) devised a surcharge loading rate to minimize the lateral displacement of vacuum PVD scheme in soft ground improvement. Moreover, Lam et al (2015) presents further analyses of field data from Vacuum PVD using numerical and analytical techniques. Figure 10 shows the data of vacuum pressures measured using the VCM-DT method.

2.2.2 Other methods of applying vacuum PVD preloading

VCM-MS method - The sand blanket is covered with an airtight membrane to enable the transfer of vacuum pressure from the sand blanket to the underlying soft soil through the PVDs. Vacuum pressures can be applied in the sand blanket through a sub-drain system using flexible perforated pipes placed at spacing of several

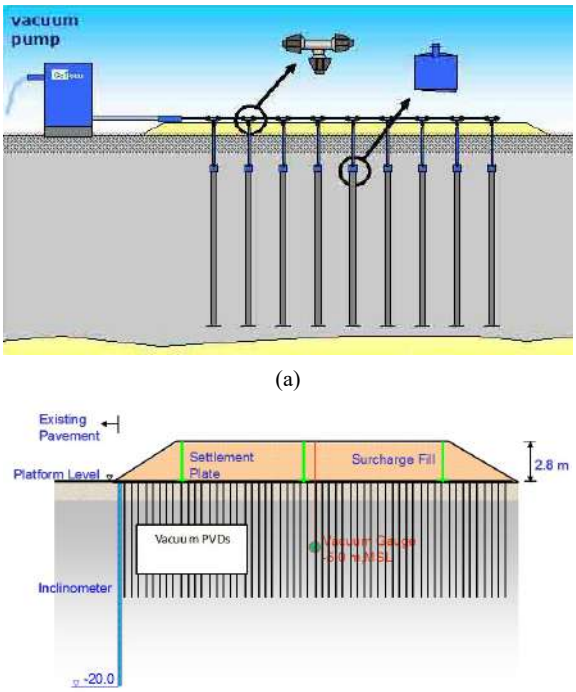

Figure 8 Vacuum PVD by direct connection method: (a) Cross-section and (b) Monitoring instruments

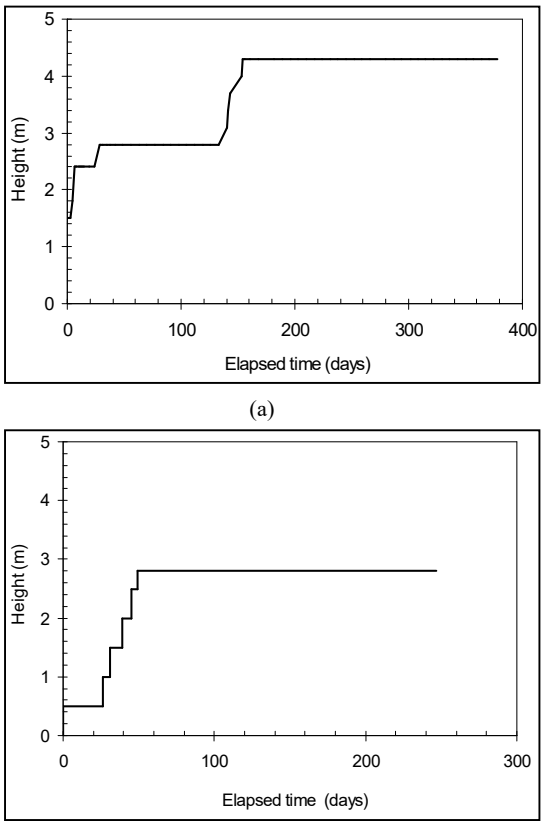

Figures 9 The load-time relationships: (a) Conventional PVD method and (b) Vacuum PVD method

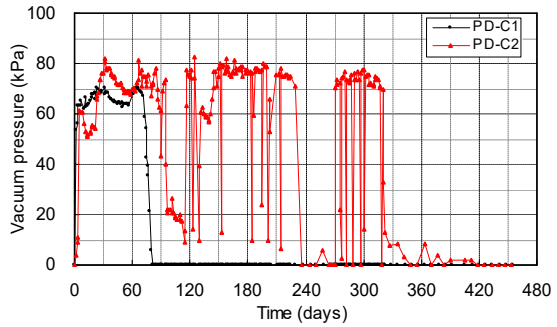

Figure 10 Measured vacuum pressure in PVDs using VCM-DT method (Long et al, 2011)

rows of PVDs. Measured data of vacuum pressures in the sand blanket as given in Figure 11 indicated that the vacuum pressure at early stage was higher than 70 kPa and then gradually decreased to about 50 to 55 kPa at the end of preloading.

VCM-MB method - Vacuum pressure can be applied to PVDs horizontal drains using perforated pipe and horizontal band drains with airtight membrane (VCM-MB) as shown in Figure 12. The measured vacuum pressures at the mid-depth of PVDs for two trial sections (D1 and D2) are presented in Figure 13. It can be seen that the effective vacuum pressure of about 70 to 80 kPa was achieved for both sections in early stages. However, after about 120 days, the vacuum pressures in Section D2 was gradually decreased to about 20 kPa at the end of preloading (EOP).

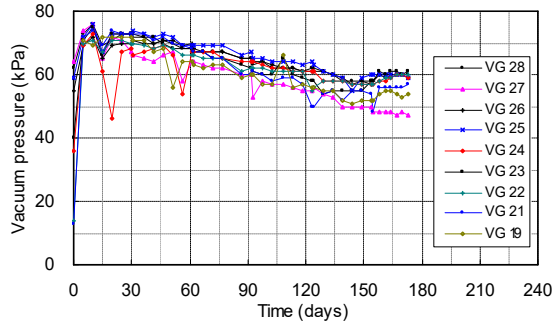

Figure 11 Measured vacuum pressure in sand blanket with airtight membrane using VCM-MS method (Long et al, 2011)

Figure 12 VCM-MB using airtight membrane and horizontal band drains (Long et al, 2011)

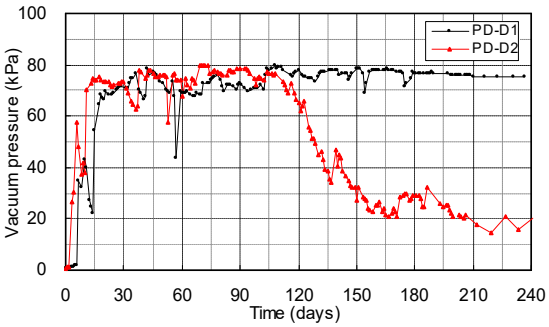

Figure 13 Measured vacuum pressures using VCM-MB method (Long et al, 2011)

VCM-MT method - For this method, horizontal drainage system under airtight membrane consisted of horizontal drainage using flexible, corrugated and perforated tubes connected to longitudinal main drains consisting of PVC or HDPE pipes. The PVDs were connected to horizontal pipes by winding with string tie (Figure 14a) and using 4-way or T-shaped connector for connection between horizontal drainage tube and longitudinal main pipe (Figure 14b). The measured vacuum pressures at the mid-depth of PVDs in various construction sections are presented in Figure 15. From this figure, it can be seen that the vacuum pressure in PVD was not dependent on the PVD lengths.

(a) Connection of PVDs to horizontal flexible pipe

(b) Connections of horizontal and longitudinal main pipe

Figure 14 VCM-MT using airtight membrane and horizontal perforated tubes (Long et al, 2011)

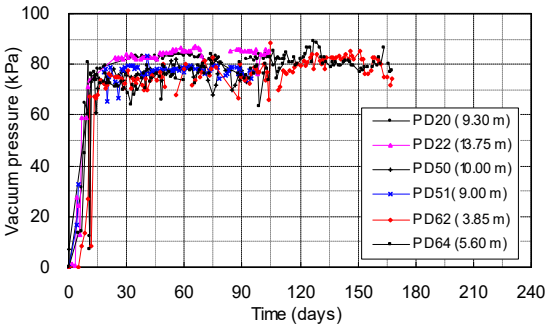

Figure 15 Measured vacuum pressures in PVDs in sections using VCM-MT method (Long et al, 2011)

2.2.3 Settlement predictions of field test using PVDs with and without vacuum

The final settlement was calculated using the Asaoka (1978) graphical method. This method is based on the field monitored data. The horizontal coefficient of consolidation, C_h, was also back-calculated at different periods depending on the time of PVD installation. Before the PVD installation, the vertical drainage was mainly assumed in the calculation of the degree of consolidation. After the PVDs installation, the horizontal drainage mainly governed in the calculation of the degree of consolidation. For the settlement analysis, the subsoil was divided into 5 layers (Table 3) and the whole surcharge fill was divided into different loading stages. The design parameters of PVDs with and without vacuum for settlement analysis are tabulated in Tables 4 and 5, respectively.

Table 4 Parameters for settlement analyses related to Vacuum PVD

Item	Unit	Values
Drain Type; CeTeau drain type CT-D911		
Equivalent diameter of the drain, $d_w = (b+t)/2$	mm	51.75
Diameter of the equivalent soil cylinder, $D_e = 1.05S$	m	0.8925
Smear zone diameter, $d_s = 2d_m$	mm	191.49
Hydraulic conductivity ratio, k_h/k_s		2-10
Discharge capacity, q_w	m^3/yr	100

Table 5 Parameters for settlement analyses related to conventional PVD

Item	Unit	Values
Drain Type; CeTeau drain type CT-D911		
Equivalent diameter of the drain, $d_w = (b+t)/2$	mm	51.50
Diameter of the equivalent soil cylinder, $D_e = 1.05S$	m	0.8925
Smear zone diameter, $d_s = 2d_m$	mm	186.00
Hydraulic conductivity ratio, k_h/k_s		2-10
Discharge capacity, q_w	m^3/yr	1000

2.2.4 Field test results using PVDs with and without vacuum pressure

The method of Asaoka (1978) for prediction of settlement magnitudes and Hansbo (1979) based on Equas. (1) to (5) for prediction of settlement rates were combined together to analyze the field observation data of two stations of PVD improved soft ground by surcharge load and another two stations of PVD improved soft ground with surcharge load combined with vacuum preloading. The measured settlements of those stations were then compared with the predictions. The comparison of settlement behavior using PVD without and with vacuum are plotted with time in Figure 16. The PVD with vacuum clearly indicates faster rate of settlements. The reduction of time to reach the 90% degree of consolidation using surcharge load combined with vacuum pressure was higher than PVDs without vacuum pressure by about 1.4 to 1.5 times due to the higher values of horizontal coefficient of consolidation. Figure 17a shows the measured and predicted settlements at station X = 14012, Y = 11567-12633 by using PVD with surcharge load. The back-calculated C_h value was 2.03 m^2/yr with k_h/k_s values of 7.0. The final settlement predicted from Asaoka method was 1485.89 mm. Figure 17b shows the measured and predicted settlements at station X = 13560, Y = 11567-12600.. The C_h value was 2.31 m^2/yr with k_h/k_s values of 7.4. The final settlement from Asaoka (1978) method was 1773.41 mm.

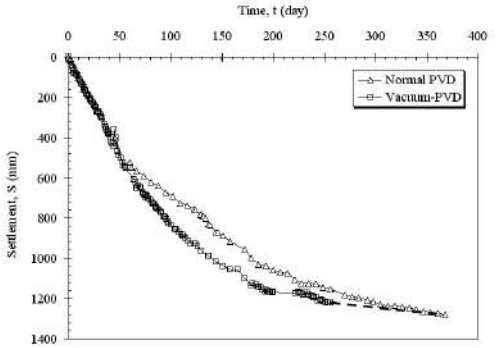

(a)

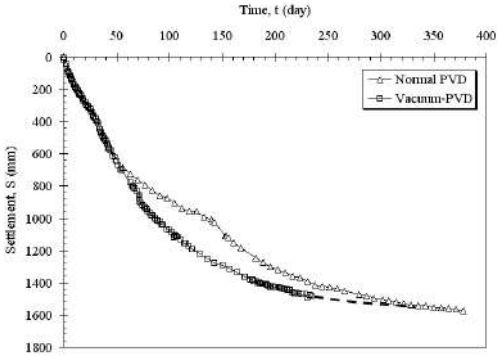

(b)

Figure 16 Comparison of settlements with time of Conventional PVD and Vacuum PVD at two sites in SBIA

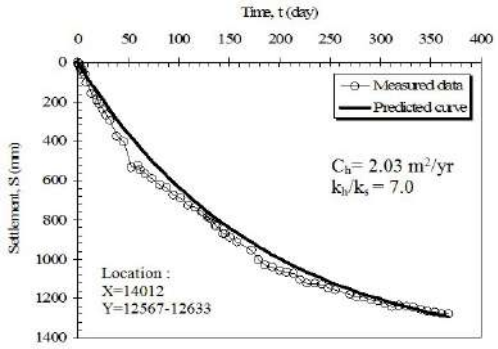

(a)

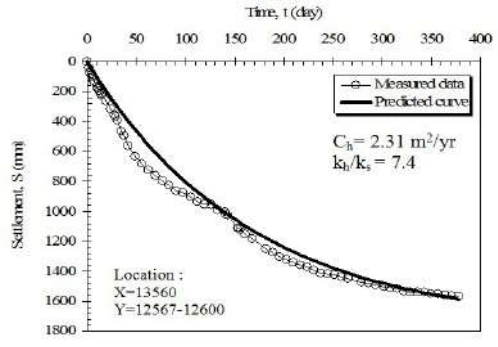

(b)

Figure 17 Back-calculation of compressibility parameters from field settlement observations of conventional PVD

Similar procedures were used in the back-calculation of compressibility parameters from measured and predicted settlements at station X = 12566.400, Y = 12570.000 by using PVD with surcharge and vacuum preloading. The C_h value was 3.21 m^2/yr with k_h/k_s values of 6.2. The final settlement predicted by Asaoka (1978) method was 1356.62 mm. The corresponding back-calculated values were also obtained from the measured and predicted settlements at another station X = 12566.400, Y = 11683.50. The back-calculated C_h value was 3.80 m^2/yr with k_h/k_s values of 7.1. The final settlement predicted by Asaoka (1978) method of the station was 1614.94 mm.

Figure 18a shows the measured and predicted settlements at station X = 12566.400, Y = 12570.000 by using PVD with surcharge and vacuum preloading. The C_h value was 3.21 m^2/yr with k_h/k_s values of 6.2. The final settlement predicted by Asaoka (1978) method was 1356.62 mm. Figure 18b shows the measured and predicted settlements at another station X = 12566.400, Y = 11683.50. The back-calculated C_h value was 3.80 m^2/yr with k_h/k_s values of 7.1. The final settlement predicted by Asaoka (1978) method of the station was 1614.94 mm.

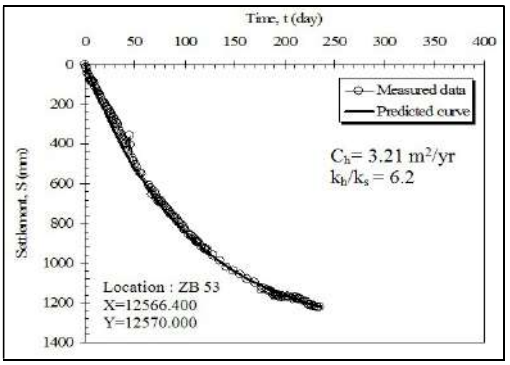

(a)

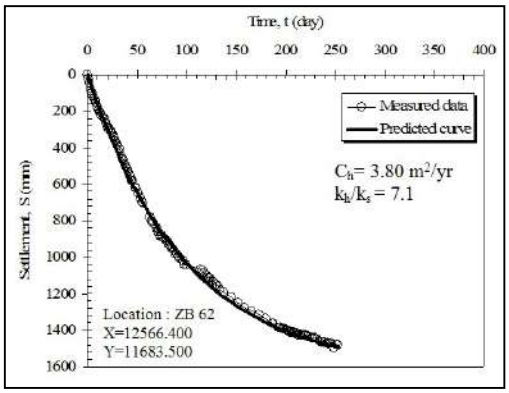

(b)

Figure 18 Back-calculation of compressibility parameters from field settlement observations of Vacuum PVD

2.2.5 PVDCON method

In PVDCON, finite element formulation consider the effects of PVDs by modifying 1D continuity equation of consolidation as follows (Chai and Miura, 2000).

$$\frac{k_v}{\gamma_w}\frac{\partial^2(u-p_{vac})}{\partial z^2}-\frac{8k_h(u-p_{vac})}{\gamma_w D_e^2\mu}+\frac{\partial\varepsilon_v}{\partial t}=0 \qquad (6)$$

$$\mu=\ln\frac{n}{s}+\frac{k_h}{k_s}\ln s-\frac{3}{4}+\pi\frac{2l^2k_h}{3q_w} \qquad (7)$$

where γ_w is the unit weight of water, z is depth, t is time ε_v is volumetric strain, u is excess pore water pressure, p_{vac} is the final vacuum pressures, k_v is hydraulic conductivity in the vertical direction, k_h is hydraulic conductivity in the horizontal direction, l is drainage length, D is the diameter of unit cell, q_w is discharge capacity of PVD, $n=D/d_w$ (d_w is the equivalent diameter of PVD) and $s=d_s/d_w$, k_h, k_s and d_s were defined previously.

For Conventional PVD, at OCR of 1.2, the k_h/k_s of 4 to 6 and $C_h=2C_v$ were obtained where C_v = 1.58 m^2/year as shown in Figure 19. For Vacuum PVD with vacuum pressure at -60 kPa, and OCR of 1.2, the k_h/k_s of 4 to 8 and $C_h=3C_v$ were obtained where C_v = 1.58 m^2/year as shown in Figure 20. In summary, the addition of vacuum pressure to PVD increased the coefficient of horizontal consolidation, C_h as expected. The other parameters may not be affected that much, particularly, the permeability ratio, kh/ks, because the vacuum preloading seems to increase both the permeabilities of the smeared and the undisturbed zones.

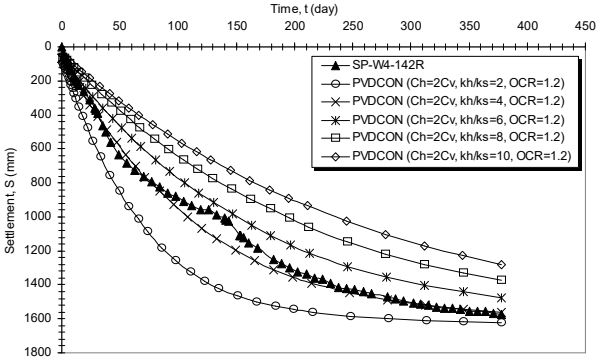

Figure 19 Observed and predicted settlements using PVDCON of Conventional PVD

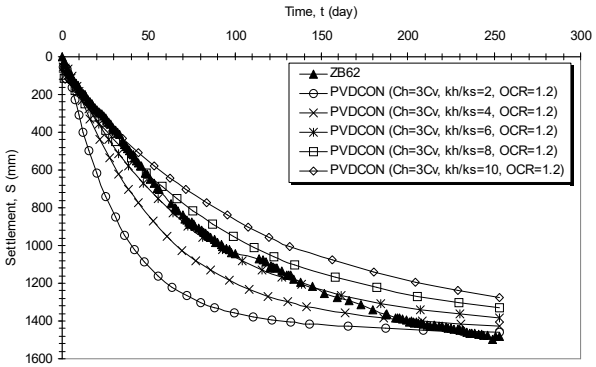

Figure 20 Observed and predicted settlements using PVDCON of Vacuum PVD

2.3 Field test using PVDs with and without heat

2.3.1 Site investigations and field construction

The embankment tests site was located inside the campus of the Asian Institute of Technology (AIT), which is 42 km north of Bangkok, Thailand. This AIT campus is located within the Central Plain of Thailand which is a flat with deltaic-marine deposits widely known as “soft Bangkok clay”. The soil profile at the site can be

divided into 3 sublayers as shown in Figure 21. It consists of a 2.0 m thick clay backfill layer overlying soft clay layer which extends from 2.0 m to 9.0 m depth. Underneath the soft clay layer, a 2.0 m thick medium clay layer can be found. The groundwater level was found at about 2.0 m depth (Bergado et al., 1990).

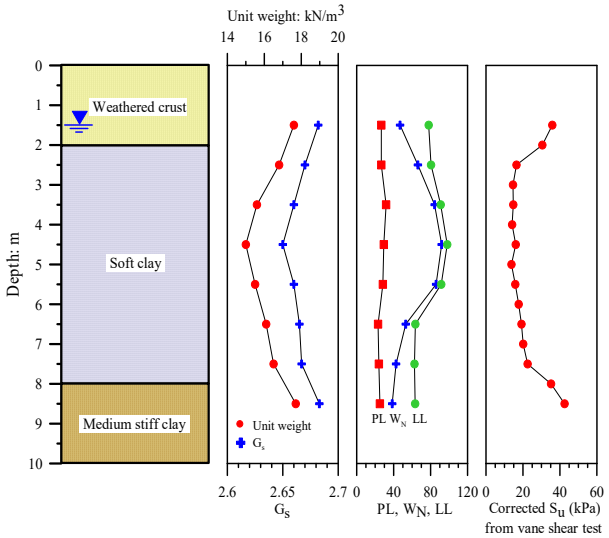

Figure 21 Soil properties at the site (AIT Campus, Thailand)

Embankments improved without and with heat using solar power were constructed in the dimensions of 11 m x 11 m at the bottom and 3 m x 3 m at the top with 6 m height as shown in Figure 22. The PVD/PVTD (Thermal PVD) was installed into 8 m depth with a spacing of 1.0 m and arranged in a square pattern.

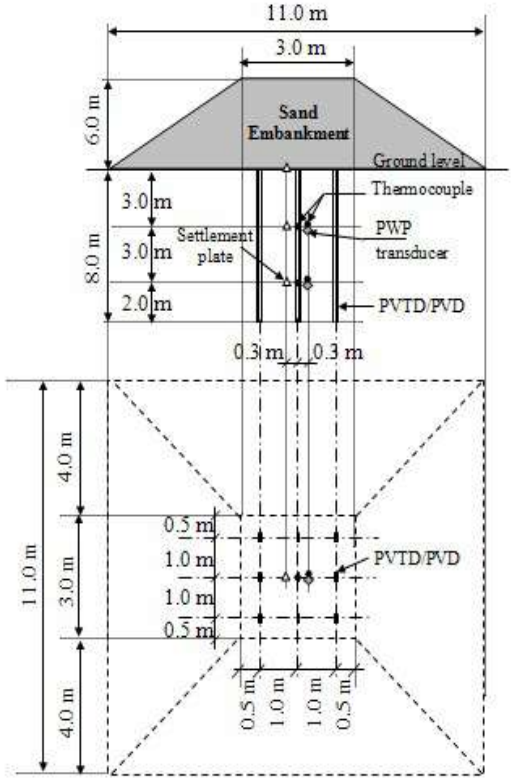

Figure 22 Layout of test embankment with thermal PVD

The embankment fill material (Ayuttaya sand) was properly compacted. Geogrid, gabion cages and geotextile were used for the slope protection. The instrumentations were installed to monitor the performances of embankments improved without and with heat using solar power. The following instrumentations were installed, namely: 2 piezometers (below 3.0 m and 6.0 m from ground surface level), 5 settlement plates (below 0.0, 3.0, and 6.0 m from ground surface level) and 4 thermo-couples (below 3.0 m and 6.0 m from ground surface level for PVTD embankment). The PVTD (Thermal PVD) unit consists of a U-tube made of cross-linked polyethylene plastic (PEX) attached to both sides of conventional PVD (Figure 23). Preheated water at about 70 to 90°C was stored in the tank and then, was circulated through the attached U-tube by water pump to raise the soil temperature underneath the embankment. A solar panel system was used to heat the circulated water from ambient temperature (25°C) to 72°C. Then an electrical heater was utilized to raise its temperature from 72°C to 90°C, especially during cloudy day and at night.

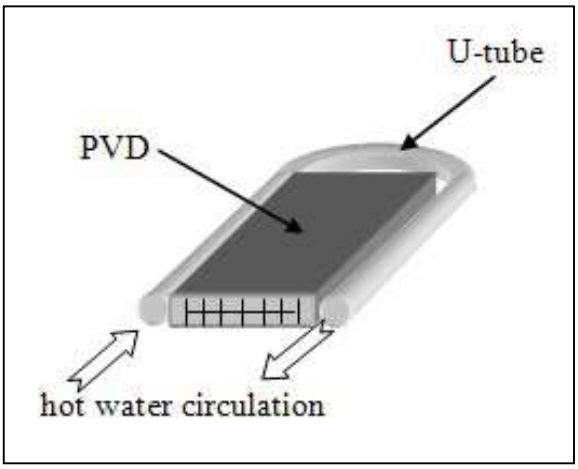

Figure 23 Configuration of Thermal PVD

2.3.2 Field test results using PVDs with and without heat

The settlement results of surface and deep settlements of two embankments with Conventional and Thermal PVD are shown in Figure 24a. Subsequently, the comparison of surface settlements from the full scale embankment improved without and with Thermal PVD is shown in Figure 24b. For the Conventional PVD embankment, the final settlement was 262.20 mm. On the other hand, the thermal PVD embankment indicated larger final settlement of 407.62 mm which had an increase of about 55%. These results demonstrate that the higher the temperature, the higher in volume contraction and the higher rate of consolidation. Thus, Thermal PVD has achieved higher settlement and also faster rate of consolidation than the Conventional PVD (Abuel-Naga et al., 2006). The compressibility increases due thermally induced irreversible contraction of underlying saturated normally consolidated (NC) soft clay. Furthermore, Abuel-Naga et al. (2006) indicated that the Thermal PVD resulted in substantial amount of settlement as much as 5 times using undisturbed specimen of soft Bangkok clay in the laboratory model test. Moreover, the compression line of soft Bangkok clay shifts to the left with approximately similar slope upon heating when thermal loading is applied at normally consolidated state. Furthermore, the normally consolidated specimens contracted irreversibly and non-linearly under drained heating condition (Abuel-Naga et al., 2007).

The excess pore pressures were measured at the embankments improved with PVD and PVTD as shown in Figure 25. For PVD embankment, the excess pore pressure had increased to maximum of

30 kPa but after 200 days decreased to about 7 kPa. For PVTD embankment had demonstrated excess pore water pressures to 30 kPa then after 200 days it reduced to 2 kPa due to the effects of thermally induced pore water pressures and volume changes. This behavior can be explained that the increase in hydraulic conductivity at elevated temperature as the result of the decrease in water viscosity. The temperature-radial distances relationship at different time of the PVTD embankment at depth of 3 m was monitored. The initial temperature was measured which showed constant temperature of 29°C at time of 0 day with T/T_0 value of 1.16 based on the standard temperature (T_0) is 25°C which is the reference temperature. The steady state condition of temperature was obtained after about 60 days and the soil temperature becomes almost constant (T/T_0=3.0) at the radial distance r/r_w of 6, where r_w is the equivalent drain radius of the Thermal PVD (PVTD) (r_w= 26 mm).

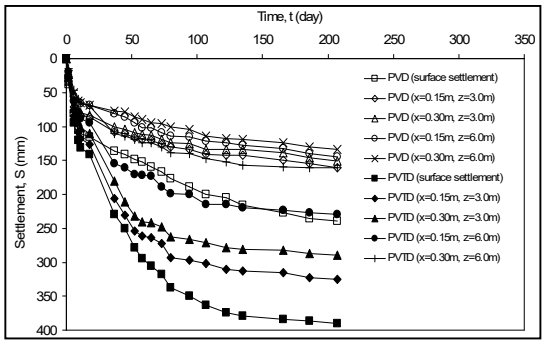

Figure 24a Surface and subsurface settlements of embankments with Conventional PVD and Thermal PVD (PVTD)

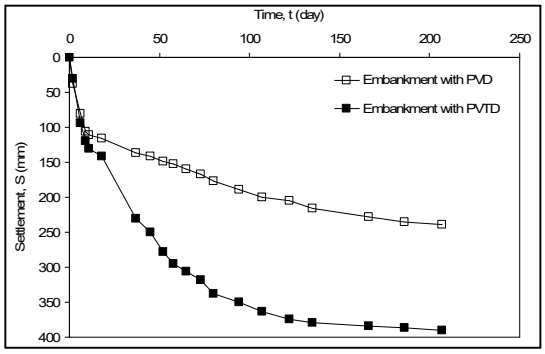

Figure 24b Surface settlements of Conventional PVD and Thermal PVD (PVTD)

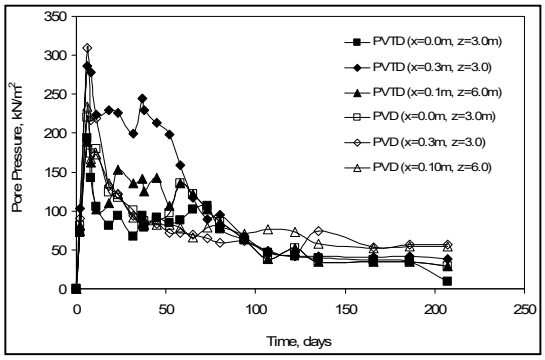

Figure 25 Excess pore pressures for Conventional PVD and Thermal PVD (PVTD)

The measured and predicted time-settlement curves for the embankment with conventional PVD and thermal PVD are shown in Figure 26. The values of C_h and k_h/k_s for the embankment with PVD only were obtained as 6.7 m^2/yr and 6.2, respectively. For the embankment with PVTD, the corresponding values were 8.5 m^2/yr and 4.1, respectively. Consequently, the use of PVTD increased the permeability of the smear zone resulting in the decrease in k_h/k_s of about 33.9% and an increase in C_h by 27.2%. Therefore, the increase in the average horizontal hydraulic conductivity beyond the smear zone is 8.5/6.7 = 1.27 times. The elevated temperature increased the horizontal permeability in the smear zone to 1.9 times as much as the horizontal permeability in the smear zone without heat.

Thus, the temperature effect on hydraulic conductivity of smear zone is higher due to the gradient behavior of heat transfer around linear heat source which generate higher temperature that coincides approximately with the smear zone (Abuel-Naga et al. 2006). Therefore, it can be concluded that Thermal PVD (PVTD) system offers a solution to partially remove the smear effect and, consequently, accelerate the consolidation process.

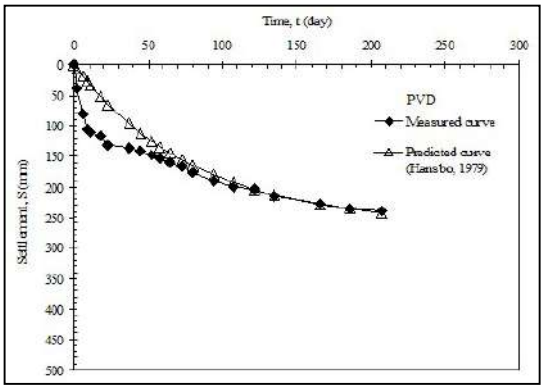

(a)

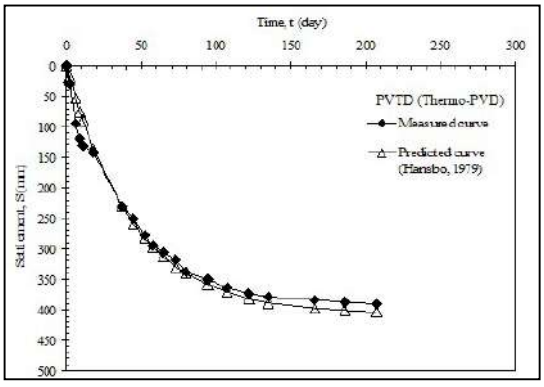

(b)

Figure 26 Back-calculation of C_h values from observed settlements: (a) Conventional PVD and (b) Thermal PVD

2.3.3 Smear effect and back-calculated C_h value

The rate of consolidation of PVD improved ground depends on PVD spacing, well resistance (F_r), and smear resistance (F_s). Well resistance is a function of PVD length and the ratio of horizontal permeability to PVD discharge capacity, k_h/q_w. The value of k_h/q_w is often smaller than 0.0001 for most PVDs in practical cases. Thus, the value of well resistance F_r becomes negligible in comparison with the values of F_n and F_s. Balasubramaniam et al. (1995), Bergado et al (2002) and Long et al (2006) also indicated that the well resistance has very little effect when the in-situ discharge

capacity of PVD greater than 50 m^3/year as seen in Figure 27. Therefore, with a known value of PVD spacing, the back-calculated C_h value mainly depends on the assumed values of $R_s = k_h/k_s$, and d_s/d_m. Moreover, with an assumed value of smear zone, d_s/d_m, the back-calculated C_h value is directly proportional to the value of R_s as seen in Figure 28 (Long et al., 2013). From this figure, it can be seen that the back-calculated value of C_h at SBIA can be varied from 1.6 m^2/year to higher than 5m^2/year depending on the assumed values of k_h/k_s and d_s/d_m. This can be explained for the different values of C_h for Nong Ngu Hao soft clay as back-calculated by various researchers (Balasubramaniam et al.,1995; Bergado et al., 2002; Long et.al, 2013).

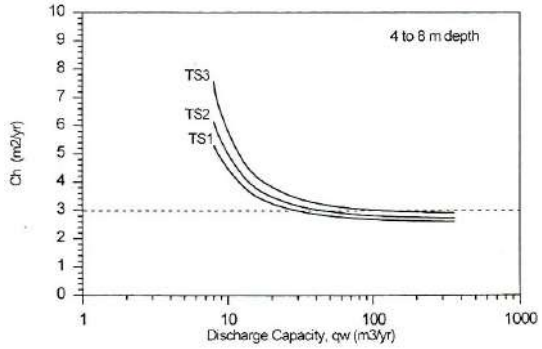

Figure 27 Back-calculated C_h value of test embankments at SBIA site using $d_s/d_m = 2$ and $k_h/k_s = 5$ (Bergado et al., 2002)

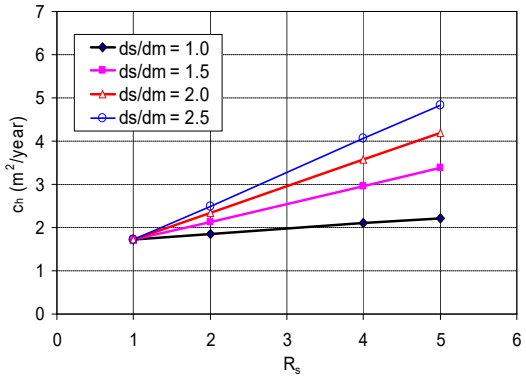

Figure 28 Back-calculated c_h values at TS3 - SBIA (Long et al., 2013)

Regarding to the smear effect under vacuum consolidation, back calculated results conducted by Long et al (2016) illustrated that the conductivity ratio, $R_s = k_h/k_s$, in vacuum consolidation is about 1.33 times smaller than that in conventional surcharge preloading. This is reasonable because under vacuum consolidation with high hydraulic gradient at the soil/PVD interface, the clogging and blinding in the PVD filter can be improved and soil particles in smear zone around PVD might be re-arranged for higher conductivity in smear zone, k_s.

2.3.4 Equivalent smear effect due to non-uniform consolidation

Zhou and Chai (2016) conducted finite element analyses (FEA) on the behavior of PVD unit cell considering only horizontal drainage and considering local variation of permeability within the unit cell. Both (a) equal stress (free strain) and (b) equal strain in the top boundary were simulated. Taylor (1948) equation was adopted for variation of permeability (k) with void ratio (e) as follows:

$$k = k_0 \cdot 10^{-(e_0 - e)/C_k} \quad (8)$$

From void ratio and initial value of k, the distributions of k at different degree of consolidation (DOC) can be calculated using Equa. (6). As illustrated in Figure 29, designate the permeability (k) at the periphery of the unit cell as k_m and at a radial distance, r, as k_r and the permeability ratio, $n=k_m/k_r$. The variation of n with radial distance is shown in Figure 30. The value of n dramatically varies within r = 100 mm and its value can be high at the early stage of consolidation. With the increase in DOC, the n value gradually decreases.

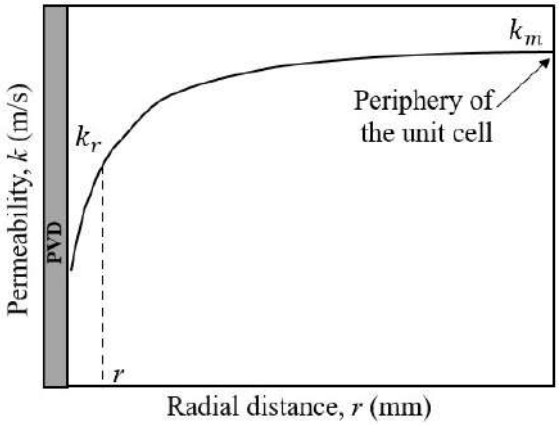

Figure 29 Illustrations of locations of k_r and k_m (Chai and Zhou, 2016)

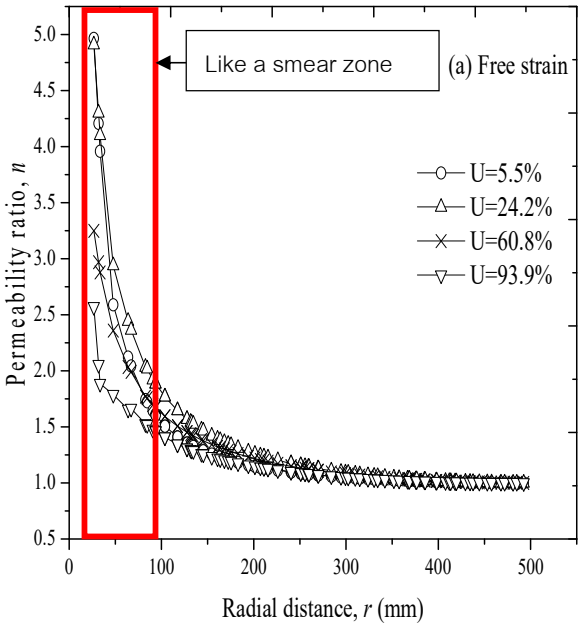

Figure 30 Permeability ratio variation with radial drainage (Chai and Zhou, 2016)

The average degrees of consolidation (DOC) are shown in Figure 31 from the results of FEA for both free and equal strain conditions where not much difference between them. The results from Hansbo (1981) without smear is also plotted for comparison. Considering a smear zone diameter, d_s, to be 4 times the equivalent diameter, d_w, of a PVD with d_s=0.21, the back-fitted $(k_h/k_s)_e$ of 2.4 is obtained. If the mechanical smear effect is denoted as $(k_h/ks)_m$ and the equivalent smear as $(k_h/k_s)_e$, then the overall smear effect, k_h/k_s, can be expressed as follows:

$$k_h/k_s = (k_h/ks)_m \times (k_h/k_s)_e \quad (9)$$

Most back-fitted field values of kh/k_s were much larger than the laboratory measured values. By separating the smear effects into mechanical component and non-uniform consolidation component, the mechanical component can be evaluated reliably. For example, the back-fitted field value of smear effect in Saga Airport, Japan was found to be $kh/k_s = 10$ by Chai and Miura (1999). However, the corresponding laboratory value obtained in the laboratory by Madhav et al (1993) was only half at $(kh/k_s)_m = 5$. Assuming the above-mentioned $(k_h/k_s)_e = 2.4$ can be used, then the overall $kh/k_s = 12$ is obtained which is close to the back-fitted value of 10. Similar values were obtained in similar situation in PVD improvement of soft Bangkok clay.

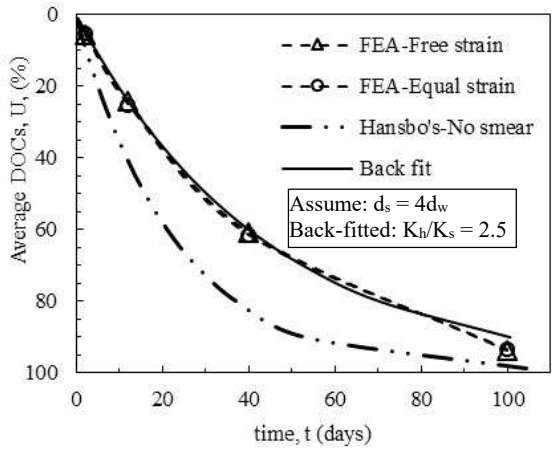

Figure 31 Comparison of average degree of consolidation (DOC) (Chai and Zhou, 2016)

3. DEEP CEMENT MIXING (DCM) and STIFFENED DCM

3.1 Prediction of shear strength and compressibility for DCM

For cement admixed clay, the shear strength and compressibility can be predicted in the laboratory tests. Figure 32 shows the relationship between the unconfined compression strength and the vertical yield stress.

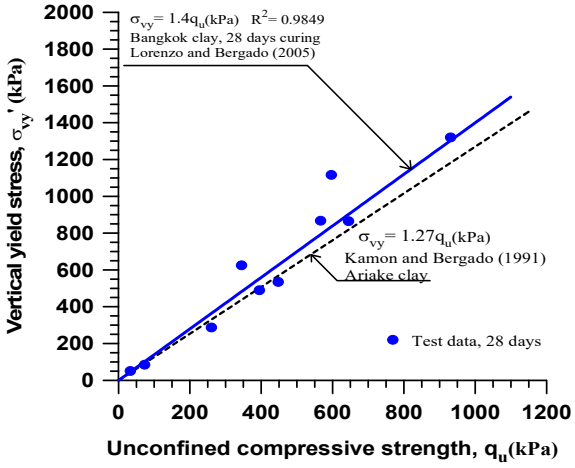

Figure 32 Relation between unconfined compression strength and vertical yield stress

For the prediction of shear strength, the ratio of after curing void ratio and cement content can be correlated with the unconfined compression strength as indicated in Figure 33. Afterwards, the data on the vertical yield stress and after curing void ratio can be combined to predict the compressibility once the post-yield compression line is established for a particular cement content (Figure 34).

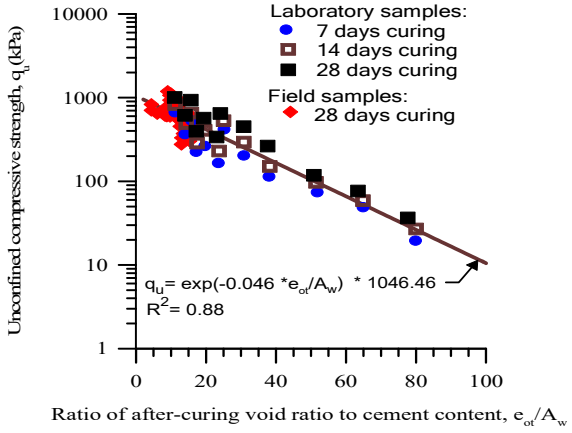

Figure 33 Unconfined compression strength versus ratio of after curing void ratio to cement content

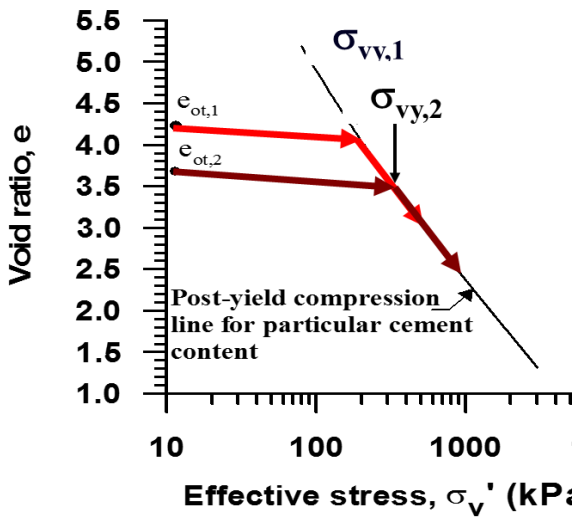

Figure 34 Relation between after curing void ratio and effective stress

3.2 Effect of curing stress on the strength of DCM

Jongpradist et al (2011) investigated the influence of curing stress on one-dimensional yielding of cement-admixed clay. The curing stress compressed the treated clay and, consequently, increased the vertical yield stress. However, the curing stress had no significant influence in the location on the post-yield compression line (Figure 34). The curing stress reduced the after curing void ratio, and subsequently, increased the shear strength of the cement-admixed clay (Figure 33).

3.3 Stiffened Deep Cement Mixing (SDCM)

Although DCM pile has many advantages with various applications, failure caused by pile failure can occur especially when subjected to the lateral loads. Moreover, the unexpected lower strength than the

design commonly occurs due to lack of quality control during construction. DCM pile can fail by pile failure mode which is lower than the soil failure mode particularly at the top of DCM pile due to low strength and stiffness as shown in Figure 35a. In addition, as shown in Figure 35b, from the test results by Petchgate et al. (2003), about half of DCM piles failed by pile failure. Consequently, the bearing capacity of DCM pile can be lower than the design load of 10 tons. Both pile and soil failures are illustrated in Figure 35a.

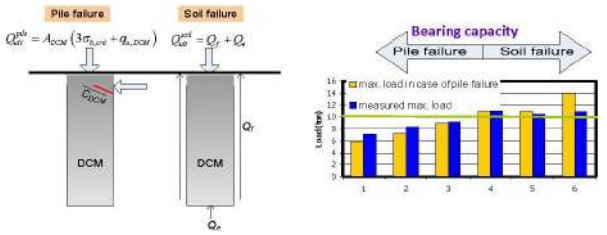

(a) (b)

Figure 35 Bearing capacity of DCM piles on soft Bangkok clay (Petchgate et al., 2003)

Stiffened Deep Cement Mixed (SDCM) piles are a composite structure of concrete piles and deep cement mixed piles combining the advantages of both components as shown in Figure 36. A pre-stressed reinforced concrete (RC) core is inserted into the center of a DCM pile immediately after the construction by wet mixing method. The two parts of the composite piles work together by supporting and transferring the vertical load effectively to the DCM pile and to the surrounding soil. In the SDCM pile, the DCM pile forms the surrounding outer layer supporting the RC core pile increasing its stiffness and resisting compressive stress along the pile.

3.4 Full scale field load and embankment tests

The full scale axial and lateral pile load tests were performed by Shinwuttiwong (2007) and Jamsawang (2008) and the full scale embankment load test was conducted by Jamsawang (2008) within

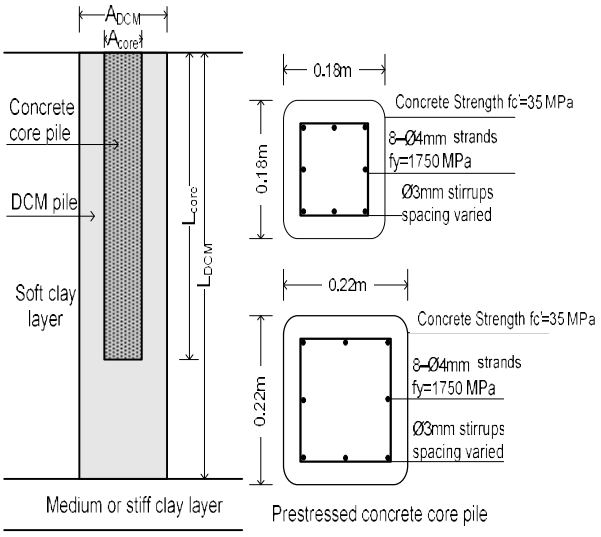

Figure 36 (a) Schematic of SDCM pile, (b) Details of prestressed concrete core piles

the campus of Asian Institute of Technology (AIT). The site is situated in the Central Plains of Thailand famous for its thick layer deposit of soft Bangkok clay. The foundation soils and their properties at the site are shown earlier in Figure 21. Other parameters are shown in Table 6. The strength of the concrete piles was found to be 35 MPa. Two lengths of concrete core piles were used in the field test, namely: 4.0 m and 6.0 m. However, for the numerical simulation the length of the concrete pile was varied from 1.00 m to 7.00 m with 1.0 m increase to evaluate the effect of the lengths of the core pile on the capacity of the SDCM pile. The Mohr-Coulomb model was recommended to simulate for mass concrete core pile instead of linear elastic model because its stiffness can be overestimated if the tensile strain is large enough to crack the concrete (Tand and Vipulandan, 2008).

Table 6 Parameters for numerical simulation.

Materials		Model	γ (kN/m^3)	Material Behavior	E'_{ref} (kPa)	v	λ^*	κ^*	c' (kPa)	ϕ' (deg)	k_x (m/day)	OCR	Tensile Strength (kPa)
Subsoil	Depth (m)												
Weathered crust	0-2.0	MCM	17	Undrained	2500	0.25			10	23	$1x10^{-3}$		
Soft clay	2.0-8.0	SSM	15	Undrained			0.10	0.02	2	23	$4x10^{-4}$	1.5	
Medium stiff clay	8.0-10.0	MCM	18	Undrained	5000	0.25			10	25	$2x10^{-4}$		
Stiff Clay	10.0-30.0	MCM	19	Undrained	9000	0.25			30	26	$4x10^{-4}$		
Foundation													
Concrete core pile		MCM	24	Drained	$2.8x10^7$	0.15			8000	40			5000
DCM pile (with interface elements)		MCM	15	Undrained	30000-60000	0.33			100-300	30	0.012	0-100	
Steel plate		LEM	-	Non-porous	$2.1x10^8$	0.15							

Note: SSM = Soft Soil Model, MCM = Mohr-Coulomb Model, LEM = Linear Elastic Model

Jamsawang (2008) and Jamsawang et al. (2008, 2009) constructed the full scale test embankment on improved soft Bangkok clay using two different method namely: stiffened deep cement mixing (SDCM) pile and deep cement mixing (DCM) pile. The DCM pile consisted of 7m long and 0.6 m in diameter. The objectives of this research work were to investigate ground improvement performances under embankment loading and to verify the related design parameters. Surface settlements and lateral movements were monitored during and after the embankment construction for two years. Figure 37 shows the plan layout of the embankment together with the DCM and SDCM piles. Figure 38 indicates the section view of the test embankment.

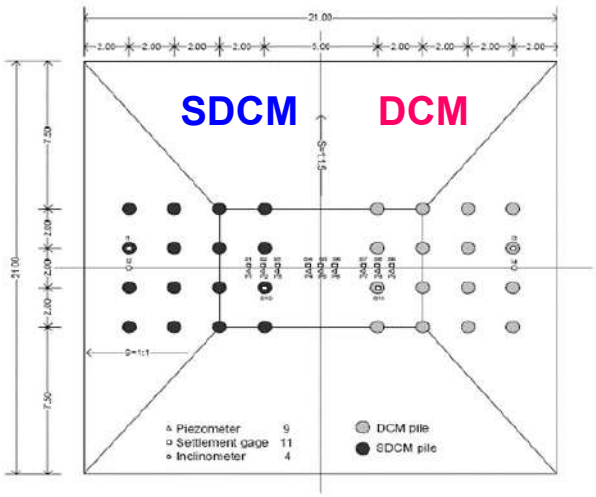

Figure 37 Plan view of the full scale test embankment test

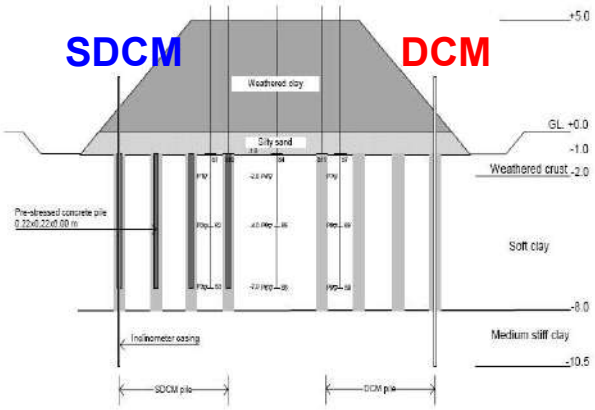

Figure 38 Section view and location of instruments of the SDCM embankment

3.5 Numerical simulations using PLAXIS 3D Foundation

The embankment is supported by two types of piles consisting of the 16-SDCM piles and 16-DCM piles. For the purpose of simulation, the length of concrete core piles in SDCM piles were varied from 3.00 to 7.00 m with varied sectional dimensions from 0.22x0.22 to 0.30x0.30 m. The embankment discretization model followed the standard procedures of PLAXIS Foundation 3D software (Brinkgreve and Broere, 2006). The soil parameters and models used in the numerical simulations are tabulated in Table 6. The soft soil model (SSM) was used for the soft clay layer and the Mohr-Coulomb model (MCM) was used for other elements including DCM and SDCM piles. The basic soil elements were represented by 15 node wedge element except the plate and interface elements. The DCM pile was modeled by volume elements that can simulate deformation stresses. The prestressed concrete core pile was modeled as "massive pile" composed of volume elements. The interface elements were modeled as pairs of corresponding nodes with zero distance between each pair. Interface elements required strength reduction factor, R_{inter}, for soil strengths mobilized at the interface. R_{inter} varies from 0.35 to 0.43 with average of 0.40 (Bhandari, 2006; Jamsawang et al, 2009; Wu et al, 2005). The first hase was the initial stage that was set-up as the in-situ state (k_0 procedure) to generate the initial in-situ stresses. In the second phase, the DCM pile and concrete core pile were installed. Next step was the excavation stage of the uppermost 1.00 m of soil. The subsequent steps consisted of filling with compacted silty sand at the first phase at the base and, subsequently, filling by compacted weathered clay. Afterwards, the surface settlement at the top of SDCM, DCM and surrounding soil were checked after 60, 90, 120, 150, 180, 240, 300, 360, 420, 510 and 600 days, respectively.

3.6 Results of full scale field tests, analyses and discussions

The surface settlements were measured at the top of DCM, SDCM piles and the unimproved ground in the middle of the embankment (untreated clay). The observed settlements are plotted in Figure 39 together with the simulated values. Both the magnitude and rate of settlements from simulations agreed well with the observed data from field tests as illustrated in Figure 39. Consequently, the parameters involved were derived and verified. The parametric study was further conducted by varying the sectional areas of the concrete core pile to 0.22 x 0.22m and 0.30 x 0.30m as well as varying the lengths of concrete core piles to 4, 5, 6 and 7m to study their effects on the embankment settlements. The effects of lengths and sectional areas of the concrete core piles of SDCM piles on the ultimate settlement of embankment simulation are illustrated in Figure 40. It can be summarized that the ultimate settlement at 600 days after consolidation proportionally decreased with increasing lengths of concrete core piles from 4 to 6m and only slightly decreased from lengths of 6 to 7m. Moreover, the ultimate settlement only slightly decreased when increasing the sectional areas of the concrete core piles from 0.22 to 0.30m.

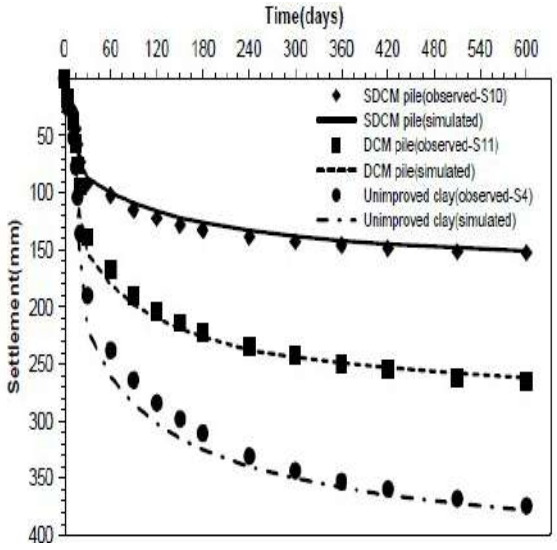

Figure 39 Comparison of observed and simulated surface settlements

Figure 41 shows the summary of the effect of core pile length on the settlement at 600 days after consolidation in surrounding clay of SDCM pile. The settlement of surrounding clay of SDCM at surface

and 4m depth decreased with increasing the lengths of concrete core pile and only slightly decreased with increasing the sectional areas. Therefore, it can be concluded that the ultimate settlements proportionally reduced with increasing lengths of concrete core pile. In addition, both the sectional area and length of concrete core pile have no effect in the subsurface settlement at 7m depth.

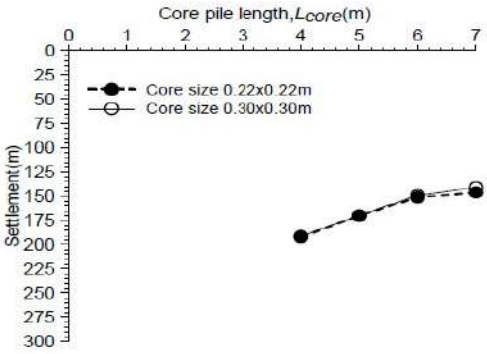

Figure 40 Effect of lengths and sectional areas of concrete core pile on ultimate settlements of SDCM pile

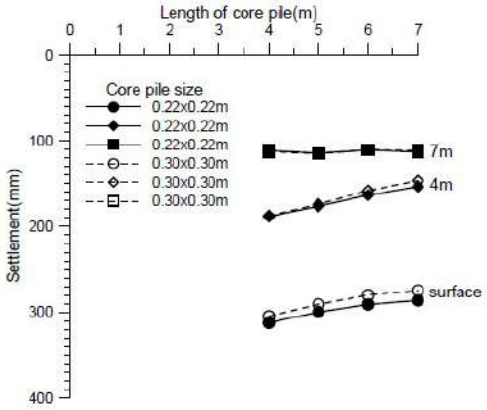

Figure 41 Effects of core pile lengths on ultimate surface and subsurface settlements in surrounding clay of SDCM pile

Differential settlements occur in the subsurface at various depths because the stresses proportionally decreased from the surface to the depths of 4 and 7m, respectively. Moreover, the stresses in the surrounding clay of SDCM and DCM piles as well as the unimproved zone are plotted together in Figure 42. The stresses of surrounding clay of SDCM is the lowest meaning that lowest settlement occur at the surface and 4 m depth. For the 7 m depth, the stresses are only slightly different and the settlements were similar.

The effect of length of concrete core pile on the lateral movements are also studied through the simulations by varying the lengths of the concrete core pile from 4 to 7m as well as their sectional areas consisting of 0.22 x 0.22 m and 0.30 x 0.30 m. The simulated and observed results of the lateral movements for both DCM and SDCM piles at different periods after construction are illustrated in Figure 43. It can be clearly observed that the lateral movements obtained from inclinometers for SDCM piles were much lower than that of DCM piles. The measured and simulated lateral movement data agreed well. The effects of concrete core pile lengths longer than 4m on lateral movements of SDCM piles, at 570 days after construction, are illustrated in Figure 44. The lateral movement reduced with increasing lengths of concrete core piles longer than 4m. From subsequent simulations as shown in Figure 45, increasing the lengths and, to a lesser degree, the sectional areas of concrete core piles, reduced the lateral movements of the SDCM piles for concrete core piles longer than 4m. The lateral movement significantly reduced with increasing lengths as well as with increasing the sectional areas of concrete core piles. It can be summarized that increasing both the lengths and sectional areas of core piles reduced the lateral movement.

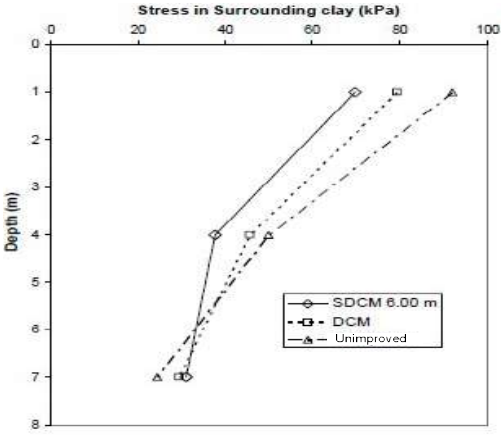

Figure 42 Stresses in surrounding clay of unimproved zone, SDCM and DCM piles piles at depth 1, 4 and 7 m

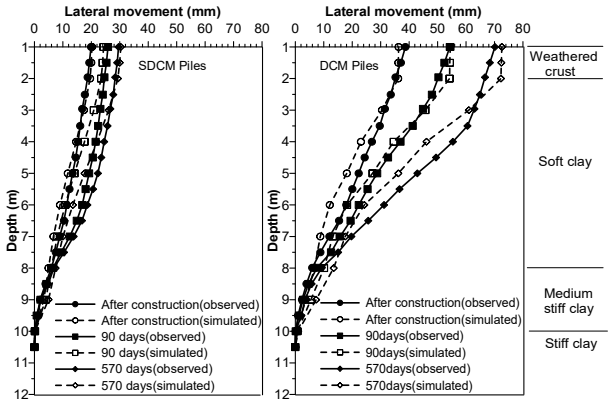

Figure 43 Simulated and observed lateral movements of SDCM and DCM piles at different periods after construction

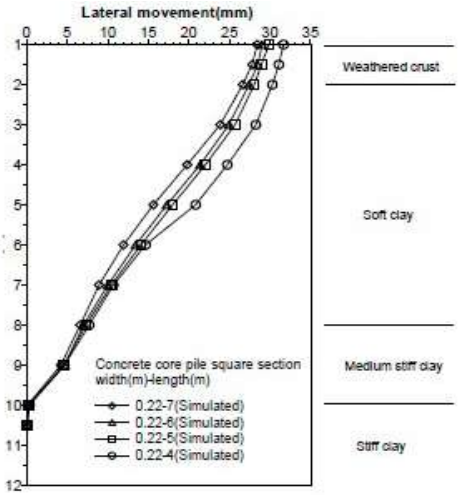

Figure 44 Effects of concrete core pile lengths on lateral movement profiles of SDCM pile with 0.22x0.22m core pile from simulations

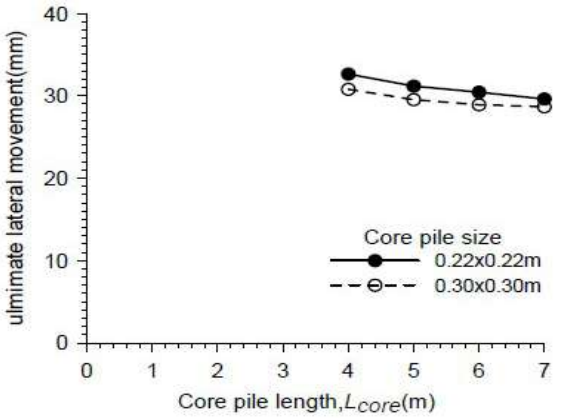

Figure 45 Effects of sectional areas and lengths of concrete core piles on the maximum lateral movement of SDCM pile

4. CONCLUSIONS

4.1 PVD method

1. Due to the increase in hydraulic conductivity of the smear zone caused by the vacuum effects, the Vacuum PVD yielded slightly lower k_h/k_s values while the coefficient of horizontal consolidation, C_h, increased. From back-calculated results of the field test data, the average C_h values were 2.17 m^2/yr. and 3.51 m^2/yr from the Conventional PVD and Vacuum PVD, respectively, with corresponding decrease in k_h/k_s values from 7.2 to 6.6.
2. The Vacuum PVD improved soft ground reduced the time to 90% degree of consolidation by one-third due to the consequent higher values of the coefficient of horizontal consolidation and subsequent increase in the rate of settlements.
3. For the Thermal PVD (PVTD) improvement, the consolidation rate was faster and the settlements was larger compared to the Conventional PVD. The permeability of the smear zone increased due to the increase in temperature which caused the reduction of viscosity in the pore water. Consequently, the k_h/k_s values slightly decreased while the coefficient of horizontal consolidation, C_h, increased.
4. The back-calculated C_h values for embankment improved with Conventional PVD and Thermal PVD (PVTD) in the field were 6.69 and 8.51 m^2/yr, respectively, and the corresponding k_h/k_s values were 6.2 and 4.1. The increased permeability in the smear zone of PVTD resulted in the decrease in k_h/k_s of about 33.9% and increase in C_h by 27.2% as well as increase in horizontal permeability in the smear zone by 1.92 times.
5. The utilization of solar heating technique in the Thermal PVD improvement of soft ground is sustainable and cost effective method to achieve the required settlement at much faster and shorter time period.

4.2 DCM/SDCM method

1. The full scale embankment loading test supported by SDCM and DCM piles was constructed, monitored and, consequently, simulated by using PLAXIS Foundation 3D finite element software in order to study and verify the design parameters.
2. The results indicated that the longer reinforced concrete (RC) core pile can reduce the vertical displacements of SDCM pile as well as the subsurface portions of the surrounding soil. The settlements reduced with increasing lengths of RC core piles from 4 to 6m but slightly reduced from 6 to 7m core pile length. Moreover, the length of RC core pile affected both the surface and subsurface settlements at 4m depth but did not affect the subsurface settlements at 7m depth.
3. In the case of lateral deformations, the lengths and sectional areas of RC core pile reduced the lateral movement of the embankment. The longer the lengths, the lower the lateral movements. Furthermore, larger sectional areas of RC core pile also reduced the lateral movements although with smaller effects. It was also found that the RC core piles need to be longer than 4 m in order to effectively reduce the lateral movements.

5. REFERENCES

Abuel-Naga, H.M., Bergado, D.T. and Chaiprakaikeow, S. (2006) "Innovative thermal technique for enhancing the performance of Prefabricated Vertical Drain during the preloading process". Geotextiles and Geomembranes, 24, pp. 359-370.

Abuel-Naga, H.M., Bergado, D.T., Bouazza, A. and Ramana, G.V. (2007) "Volume change behavior of saturated clays under drained heating conditions: Experimental results and constitutive modelling", Canadian Geotechnical Journal, 44, pp. 942-956.

Abuel-Naga, H.M., Bergado, D.T., and Bouazza, A. (2008) "Thermal conductivity evolution of saturated clay under consolidation process". International Journal of Geomechanics, ASCE, 8, No.2, pp. 114-122.

Abuel-Naga, H.M. and Bouazza, A. (2009) "Equivalent diameter of a Prefabricated Vertical Drain". Geotextiles and Geomembranes, 27, pp. 227-231.

Abuel-Naga, H, Bergado, DT and Gniel, J. (2015). "Design chart for PVD improved ground".Geotextiles and Geomembranes,43, No 6.

Asaoka, A. (1978) "Observational procedure of settlement prediction". Soils and Foundations, 18, No.4, pp. 87-101.

Balasubramaniam, A.S., Bergado, D.T. and Phienwej, N. (1995) The Full Scale Field of Prefabricated Vertical Drains for the Second Bangkok Airport, Final Report, Division of Geotechnical and Transportation Engineerinf, AIT, Bangkok, Thailand, 259 pages.

Bhandari, A. (2006) Laboratory Investigation of Stiffened Deep Cement Mixed (SDCM) Pile. M.Eng. Thesis No. GT-78-6, Asian Institute of Technology (AIT), Bangkok, Thailand.

Bergado, D.T., Ahmed, S., Sampaco, C.L. and Balasubramaniam, A.S. (1990). "Settlement of Bangna-Bangpakong Highway on soft Bangkok clay". ASCE Journal of Geotechnical Engineering, 116, No.1, pp. 136-154.

Bergado, D.T., Asakami, H., Alfaro, M. and Balasuramaniam, A. S. (1991). "Smear effects of vertical drains on soft Bangkok clay". Journal of Geotechnical Engineering, ASCE, 117, No.10, pp. 1509-1529.

Bergado, D.T., Balasubramanian, A.S., Fannin, R.J., and Holtz, R.D. (2002) "Prefabricated Vertical Drain (PVD) in soft Bangkok clay: A case of NBIA Project". Canadian Geotechnical Journal, 39, No.2, pp. 304-315.

Brinkgreve, R.B. and Broere, W. (2006) PLAXIS 3D Foundation Version 1.6 Manual. Balkema, A. A., Rotterdam, Brookfield, Netherlands.

Chai, J.C. and Miura, N. (1999) "Investigations of factors affecting vertical drain behaviour". ASCE J. of Geotech. and Geoenvi. Engg". 125, No. 3, pp. 216-226.

Chai, J.C., Carter, J.P. and Hayashi, S. (2006) "Vacuum consolidation and its combination with embankment loading". Canadian Geotechnical Journal, 43, pp. 985-996.

Chai, J.C., Miura, N. and Nomura, T. (2007) "Experimental investigation on optimum installation depth of PVD under vacuum consolidation". Proceedings 3rd China-Japan Joint Geotecnical Symposium, China.

Chai, J.C. and Rondonuwu, S.G. (2015) "Surcharge loading rate for minimizing lateral displacement of PVD improved deposit with vacuum pressure". Geotextiles and Geomembranes, 43, No. 6.

Chai, J.C. and Zhou, Y. (2016) "Equivalent smear effect due to non-uniform consolidation around a PVD." Goetechnique, pp. 1-10 [http://dx.doi.org/10.1680/jgeot.16.P.087].

COFRA (Thailand) (1996) Design and Proposal for the Execution of a Test Field: Vacuum Consolidation for the Landslide Road System for Second Bangkok International Airport, Bangkok, Thailand.

Hansbo, S. (1979) "Consolidation of clay by band-shaped prefabricated drains". Ground Engineering, 12, No.5, pp. 16-25.

Hansbo, S. (1981) "Consolidation of fine-grained soils by prefabricated drains". Proc. 10th International Conference on Soil Mechanics and Foundation Engineering, Stockholm, 1, pp. 677-682.

Indraratna, B., Rujikatkamjorn, C., and Sathananthan, L. (2005) "Analysis and numerical solution for a single vertical drain including effects of vacuum preloading". Canadian Geotechnical Journal, 42, pp. 994-1014.

Jamsawang, P. (2008) Full Scale Tests on Stiffened Deep Cement Mixing (SDCM) Pile Including 3d Finite Element Simulation. D. Eng. Diss. No. GE-08-01, Asian Institute of Technology, Bangkok, Thailand.

Jamsawang, P., Bergado, D.T., Bandari, A. and Voottipruex, P. (2008) "Investigation and simulation of behavior of stiffened deep cement mixing (SDCM) piles". International Journal of Geotechnical Engineering, 2, No.3, pp.229-246.

Jamsawang, P., Bergado, D.T., Bhandari, A. and Voottipruex, P. (2009) "Behavior of Stiffened Deep Cement Mixing (SDCM) pile in laboratory". Lowland Technology International, June, 2009.

Jongpradist, P., Youwai, S., Manorat, S., Kongkitkul, W. and Chucheepkul, S. (2011) "Influence of curing stress on one-dimensional yielding of cement-admixed Bangkok clay at high water content", Soil and Foundations, 51, No. 2, pp. 351-357.

Kjellmann, W. (1952). "Consolidation of clay soil by means of atmospheric pressure". Proc. on Soil Stabilization Conference, Boston, U.S.A., 1, pp. 258-263.

Lam, L.G., Bergado, D.T., and Hino, T. (2015) "PVD improvement of soft Bangkok clay with and without vacuum preloading using analytical and numerical analyses". Geotextiles and Geomembranes, 43, No.6, pp. 547–557.

Long, P.V., Bergado, D.T., Nguyen, L.V., and Balasubramaniam, A.S. (2011) "Design performance of soft ground improvement using PVD with and without vacuum consolidation". Proc. Intl. Symp. on Sustainable Geosynthetics and Green Technology for Climate Change, Bangkok, Thailand, pp. 1-21.

Long, P.V., Bergado, D.T., Nguyen, L.V. and Balasubramaniam, A.S. (2013) "Design and performance of soft ground improvement using prefabricated vertical drains with and without vacuum consolidation". Geotechnical Engineering Journal of SEAGS & AGSSEA, 44, No. 4, pp. 37-52.

Long, P.V., Nguyen, L.V., Bergado, D.T. and Balasubramaniam, A.S. (2015). "Performance of PVD improved soft ground using vacuum consolidation method with and without airtight membranes". Goetextiles and Geomembranes, 43, No. 6, pp. 473–483.

Long, P.V., Nguyen, L.V., Tri, T.D. and Balasubramaniam, A.S. (2016). Performance and Analyses of Thick Soft Deposit Improved by PVD with Surcharge Preloading and Vacuum Consolidation – A Case Study at CMIT, Proceedings 11th SEAGS-2nd AGGSEA Conference, Kuala Lumpur, Malaysia.

Madhav, R., Park, Y.M. and Miura, N. (1993) "Modeling and study of smear zones around band shaped drains". Soils and Foundations, 33, No. 4, pp. 135-147.

Mohamedelhassan, E. and Shang, J.Q. (2012 "Vacuum and surcharge combined one-dimensional consolidation of clay soils". Canadian Geotechnical Journal, 39, pp. 1126-1138.

Petchgate, K., Jongpradist, P. and Panmanajareonphol, S. (2003). Field pile load test of soil-cement column in soft clay. Proceedings of the International Symposium 2003 on Soil/Ground Improvement and Geosynthetics in Waste Containment and Erosion Control Applications, *2-3* December 2003, Asian Institute of Technology, Thailand, pp. 175-184.

Pothiraksanon, C., Saowapakpiboon, J., Bergado, D.T. and Thann, N.M. (2008) "Reduction of smear effects around PVD using Thermo-PVD". Ground Improvement, 161, (G14), pp. 179-187.

Pothiraksanon, C., Saowapakpiboon, J., Bergado, D.T., Voottipruex, P and Abuel-Naga, H. (2010) "Soft ground improvement with PVD and Thermo PVD with solar power". Ground Improvement Journal, 163, Issue G11, pp. 1-8.

Saowapakpiboon, J., Bergado, D.T., Thann, Y.M., Voottipruex, P. (2009) "Assessing the performance of PVD with vacuum and heat preloading". Geosynthetics International, 16, No.5, pp. 384-392.

Saowapakpiboon, J., Bergado, D.T., Youwai, S., Chai, J.C., Wanthong, P., and Voottipruex, P. (2010) "Measured and predicted performance of Prefabricated Vertical Drains (PVDs) with and without vacuum preloading". Geotextiles and Geomembranes, 28, pp. 1-11.

Shinwuttiwong, W. (2007) Full Scale Behavior of SDCM Piles under Axial and Lateral Loading with Simulations, M. Eng. Thesis No GE-07-04, Asian Institute of Technology, Bangkok, Thailand.

Suksawat, T. (2009) Numerical Simulation of SDCM and DCM Piles under Axial and Lateral Loads and under Embankment Load: A Parametric Study. M. Eng. Thesis No. GE-08-09, Asian Institute of Technology, Bangkok, Thailand.

Tand, K.E. and Vipulanandan, C. (2008) Comparison of Computed vs. Measured Lateral Load/Deflection Response of ACIP piles. PLAXIS Bulletin, Issue 23, pp. 10-13.

Wu, M., Zhao, X. and Dou, Y.M. (2005) "Application of stiffened deep cement mixed column in ground improvement". Proceedings Intl. Conf. on Deep Mixing Best Practices and Recent Advances, Stockholm, Sweden.